

Supported by



Measurement and Analysis of Core Turbulence in NSTX

S. Kubota, W. A. Peebles, N. A. Crocker, X. V. Nguyen

Institute of Plasma and Fusion Research, UCLA

D. R. Mikkelsen, R. E. Bell, S. M. Kaye,

B. P. LeBlanc, G. J. Kramer, E. J. Valeo

Princeton Plasma Physics Laboratory

C. E. Bush

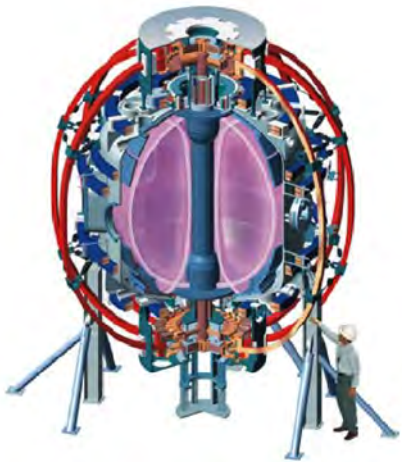
Oak Ridge National Laboratory

47th Annual Meeting of Division of Plasma Physics

American Physical Society

October 24-28, 2005

Denver, CO



*Columbia U
Comp-X
General Atomics
INEL
Johns Hopkins U
LANL
LLNL
Lodestar
MIT
Nova Photonics
NYU
ORNL
PPPL
PSI
SNL
UC Davis
UC Irvine
UCLA
UCSD
U Maryland
U New Mexico
U Rochester
U Washington
U Wisconsin
Culham Sci Ctr
Hiroshima U
HIST
Kyushu Tokai U
Niigata U
Tsukuba U
U Tokyo
JAERI
Ioffe Inst
TRINITI
KBSI
KAIST
ENEA, Frascati
CEA, Cadarache
IPP, Jülich
IPP, Garching
U Quebec*

Measurement and Analysis of Core Turbulence in NSTX¹

S. Kubota, W.A. Peebles, N.A. Crocker, X.V. Nguyen (UCLA)
D.R. Mikkelsen, R.E. Bell, S.M. Kaye, B.P. Leblanc,
G.J. Kramer, E.J. Valeo (PPPL)

Measurements of core turbulence using a homodyne radial correlation reflectometer (26-40 GHz) and quadrature reflectometers (30, 42, 49.8 GHz) have been made in NSTX discharges (Ohmic, NB, RF heated L-modes, and Ohmic H-modes) which have peaked low density profiles for good core access. Previous measurements of NB-heated L-mode discharges indicated radial correlation lengths (L_{cr}) increasing from ~2 to 10-15 cm over a radius from $\rho \sim 0.7$ to 0.4. This range of values is typical for most L-mode discharges observed. However for Ohmic H-mode discharges, a sudden decrease in L_{cr} in the core plasma is seen at the L-H transition. Analysis of the reflectometer data will be aided by the use of a fast 2-D full-wave code [E.J. Valeo, G.J. Kramer, R. Nazikian, Plasma Phys. Control. Fusion 44, L1 (2002)]. The long-term goal is a direct comparison between experimental results and turbulence predictions using the non-linear gyrokinetic simulation code GYRO.

¹Supported by U.S. DoE Grant DE-FG03-99ER54527.

Goals and Poster Content



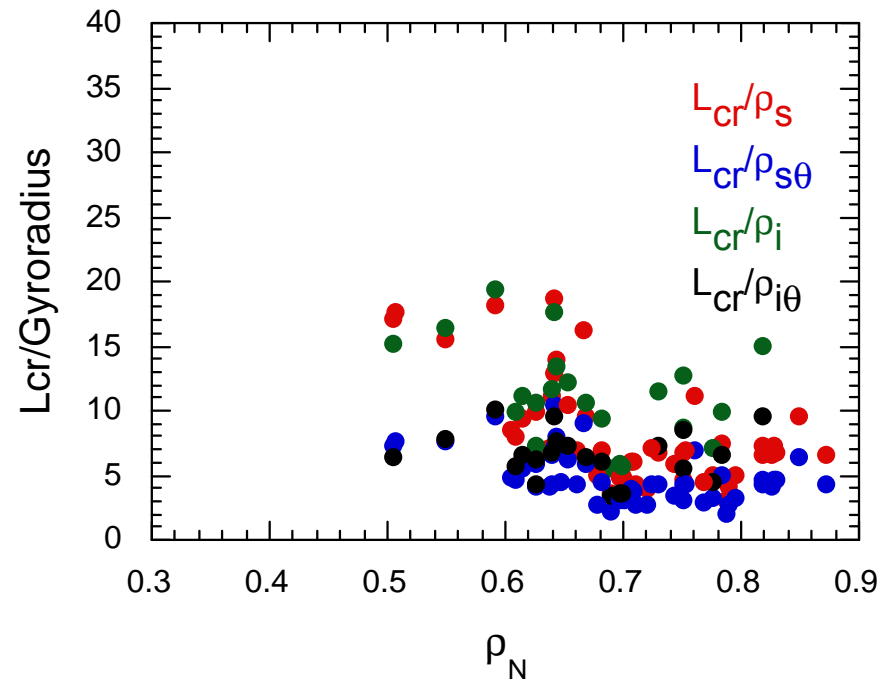
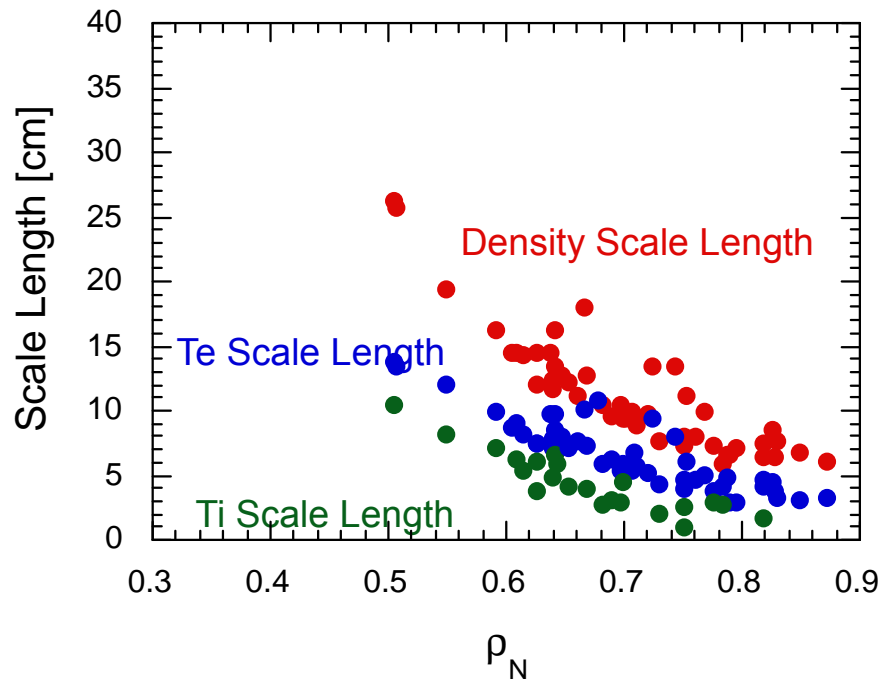
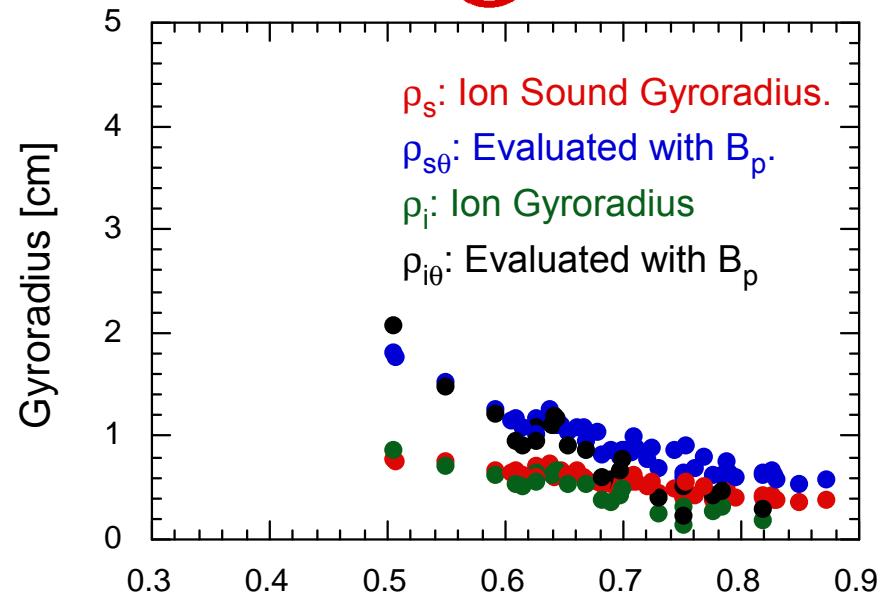
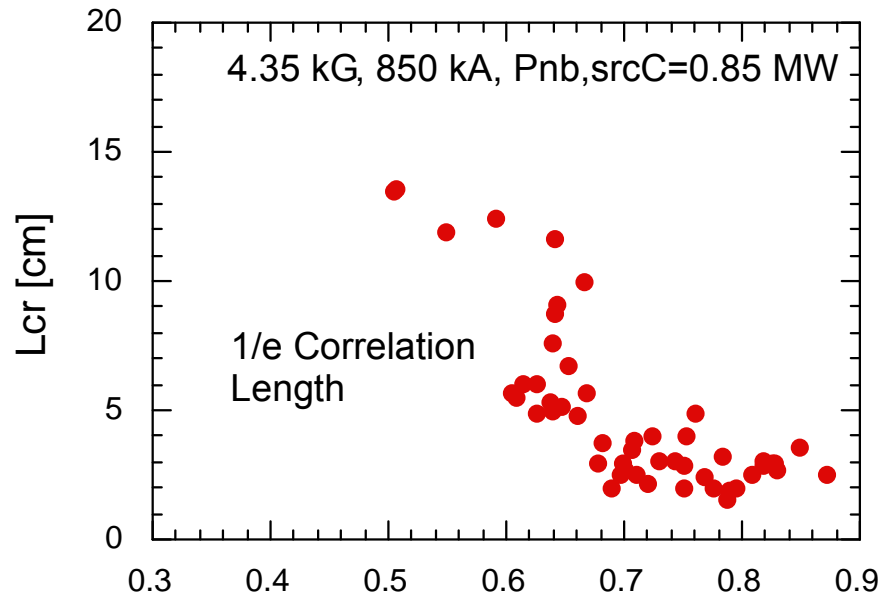
- Overview of correlation length measurements in various NSTX L-mode discharges (NB-heated, RF-heated, He Ohmic).
- Estimates of $\delta n/n$ and L_{cr} are made by comparing correlation and quadrature reflectometry data from results of full-wave simulations.
 - 1-D full-wave code to evaluate linear mode (O-X) conversion due to magnetic shear.
 - 2-D full-wave code with simulated turbulence to quantify $\delta n/n$ and L_{cr} .
 - Validate homodyne (versus quadrature) correlation.
- *Ohmic H-mode discharges show first direct connection between core turbulence properties and confinement.*
- Current and planned reflectometer capabilities on NSTX. Future work.

Background and Previous Results

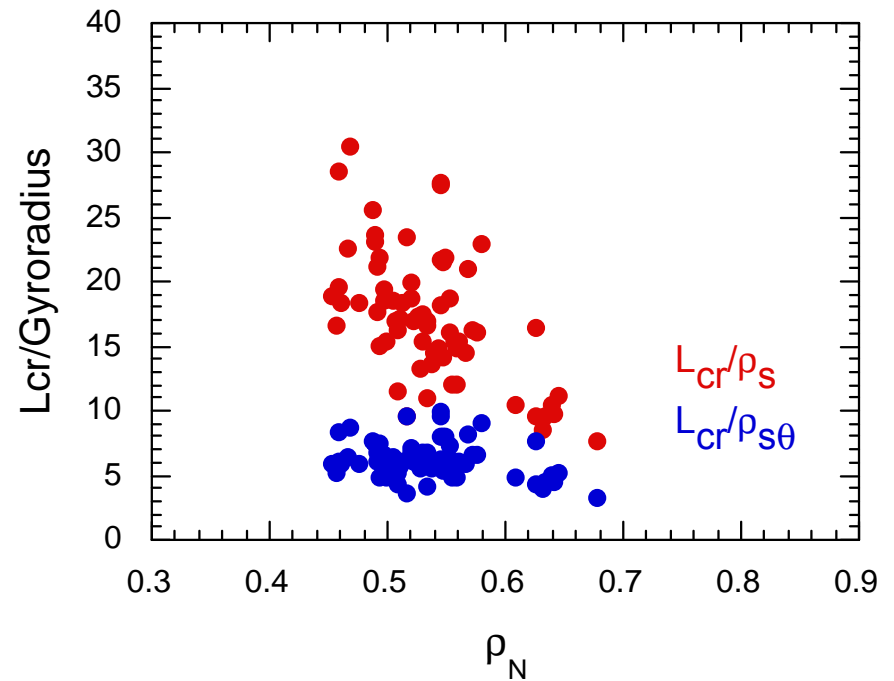
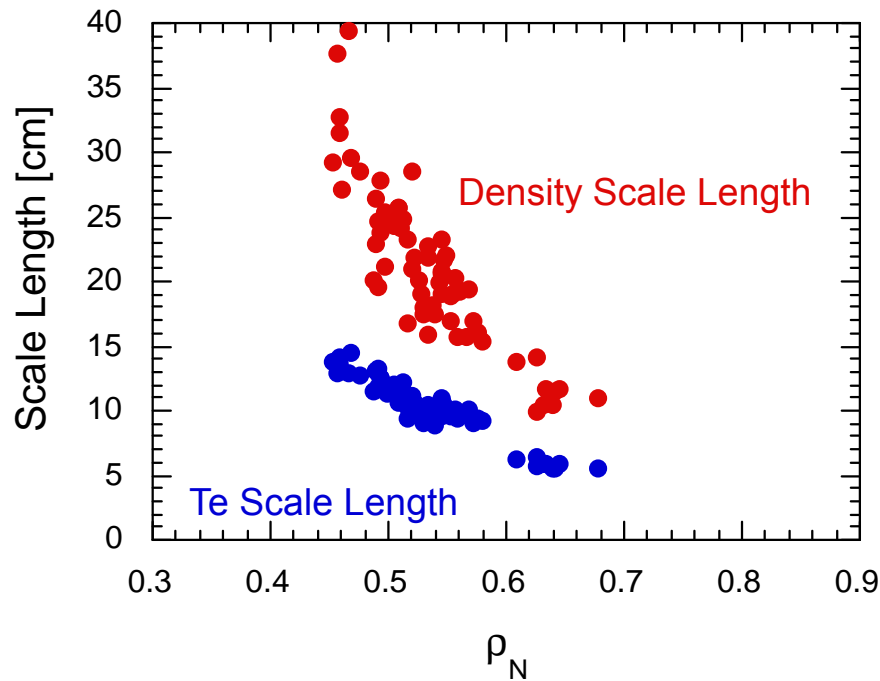
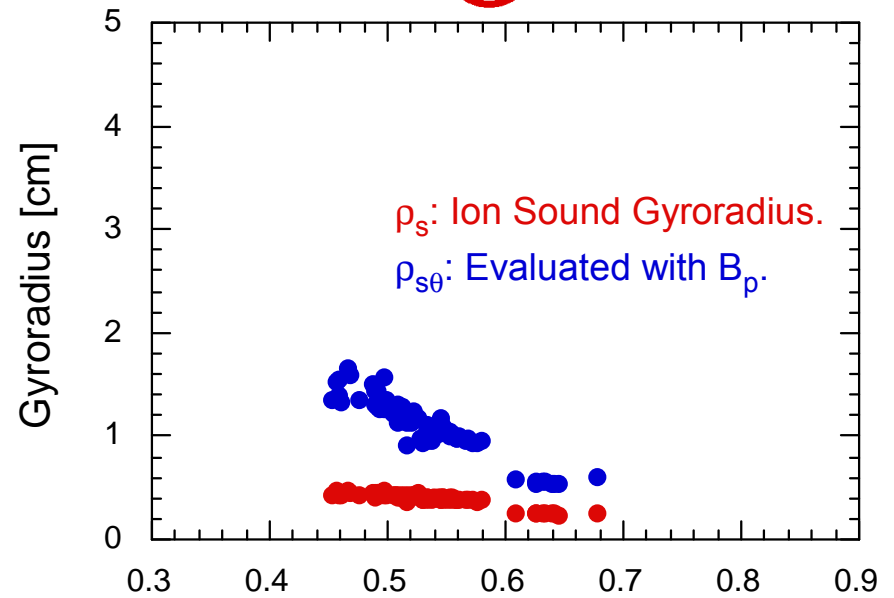
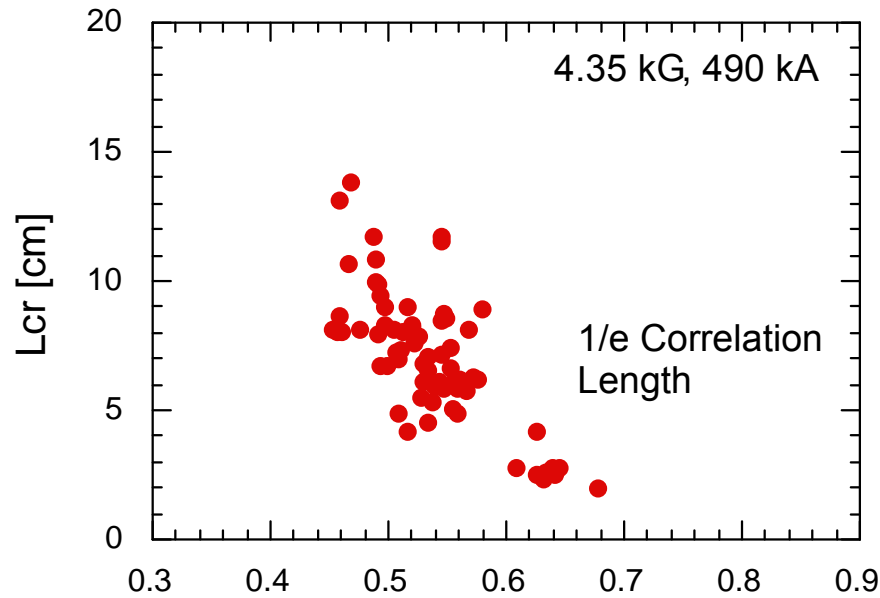


- Core transport of long wavelength turbulence (ITG modes, TEM's, micro-tearing modes with $k_{\theta}\rho_s \leq 1$) thought to be suppressed due to increased $E \times B$ shear, T_i/T_e ratio and gradient β effects.
- Assessment of thermal transport for NB-heated discharges via TRANSP often indicate low levels for the ion channel. Connection with turbulence is indirect (linear gyrokinetic stability analysis).
- Recently, reflectometry measurements have focused on measuring density fluctuation levels and radial correlation lengths for low density L-mode discharges.
 - 30, 42, and 49.8 GHz quadrature channels.
 - 26-40 GHz homodyne radial correlation system.
- Correlation lengths are calculated from 1/e decorrelation distance of homodyne signals and show similar values over a wide variety of discharges (NB- and RF-heated, He Ohmic). Typical results:
 - Correlation lengths increase from ~ 2 cm near edge to ~ 10 - 20 cm in core. These values are ~ 5 - $20\rho_s$.
 - Actual density turbulence correlation lengths can be different.
- The present study focuses on using 1-D and 2-D full wave codes to determine reflectometer response to plasma turbulence.

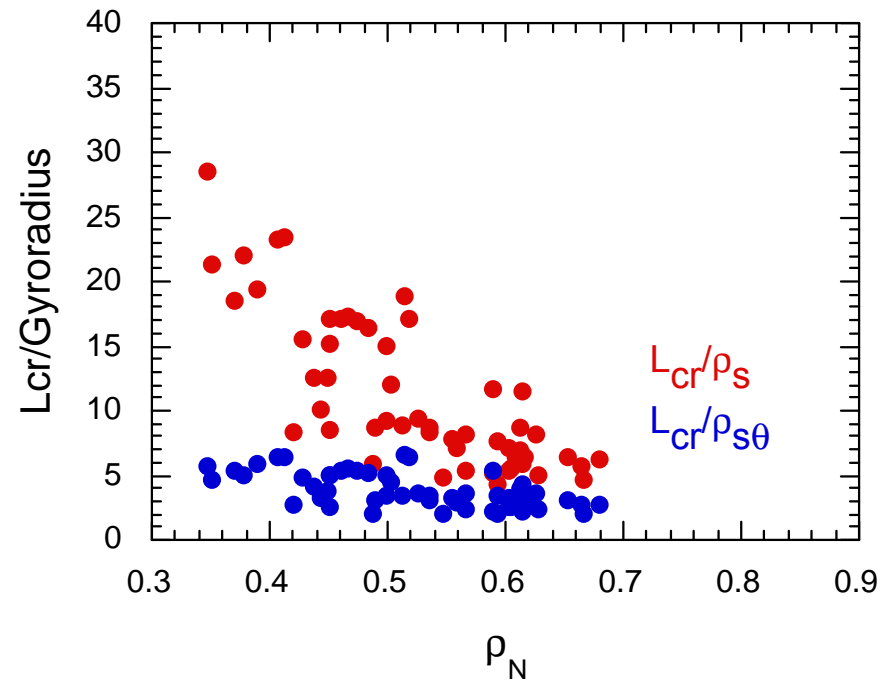
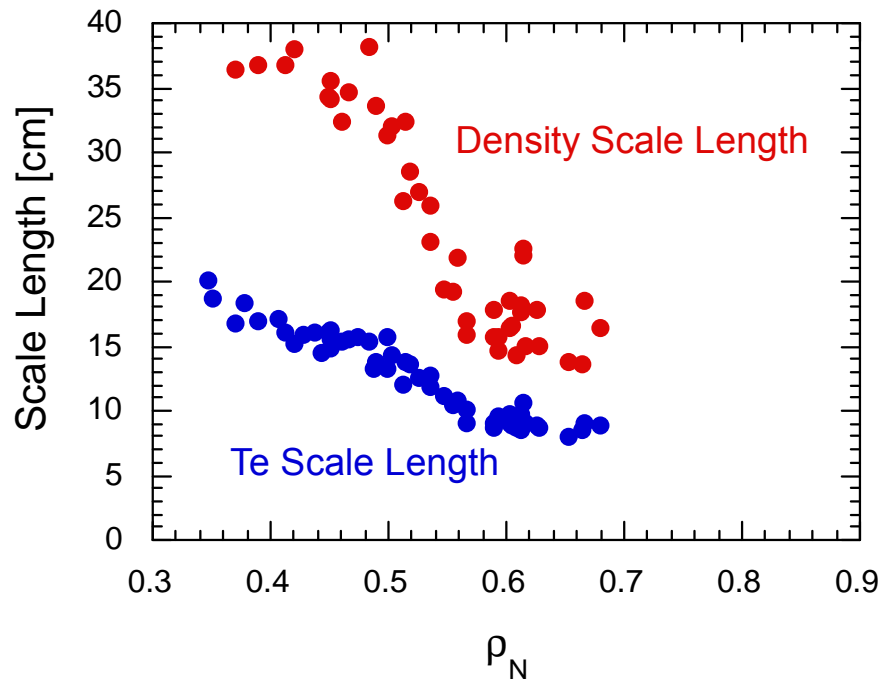
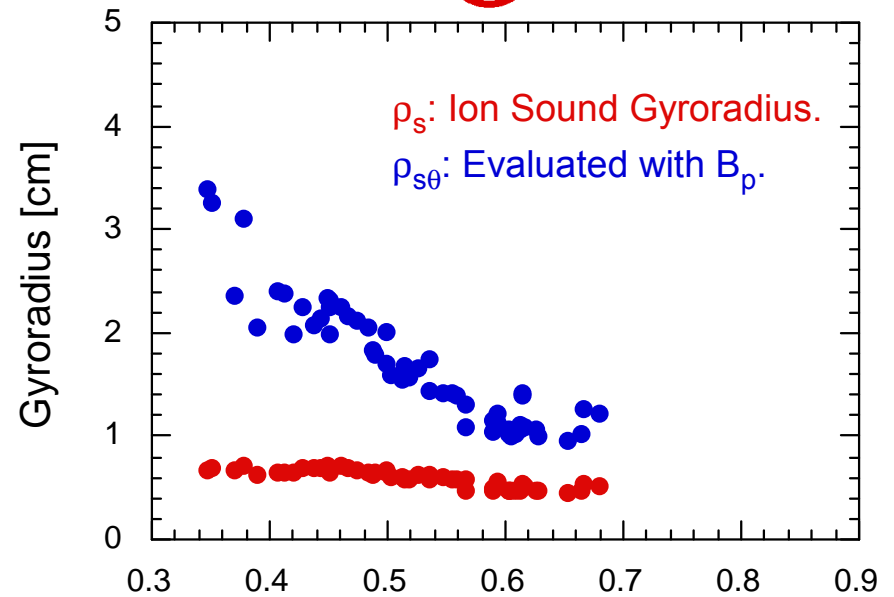
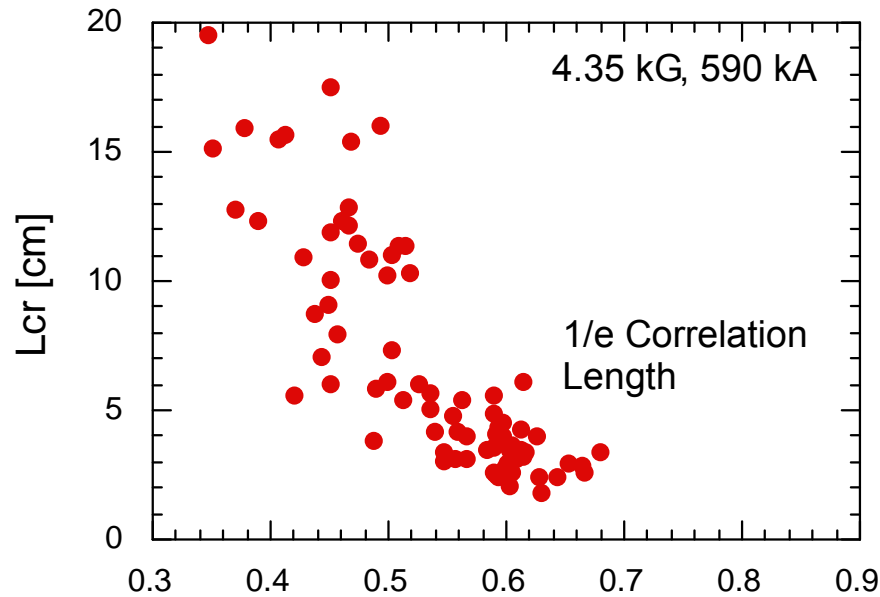
Radial Correlation Length (L_{cr}) for NB-Heated Discharges



Radial Correlation Length (L_{cr}) for Ohmic He Discharges



Radial Correlation Length (L_{cr}) for RF-Heated Discharges



Signal Contamination Due to Linear Mode Conversion



- For devices such as the ST, RFP, and helical devices with large magnetic shear, **polarization mismatch** and/or **linear mode conversion** due to magnetic shear can cause signal contamination.
- O-mode and X-mode are coupled by magnetic shear:

$$\frac{d^2 E_{\parallel}}{dz^2} + (k_0^2 N_O^2 - \phi^2) E_{\parallel} = 2\phi \frac{dE_{\perp}}{dz} + \frac{d\phi}{dz} E_{\perp}$$

$$\frac{d^2 E_{\perp}}{dz^2} + (k_0^2 N_X^2 - \phi^2) E_{\perp} = -2\phi \frac{dE_{\parallel}}{dz} - \frac{d\phi}{dz} E_{\parallel}$$

E_{\parallel}, E_{\perp} : electric field components

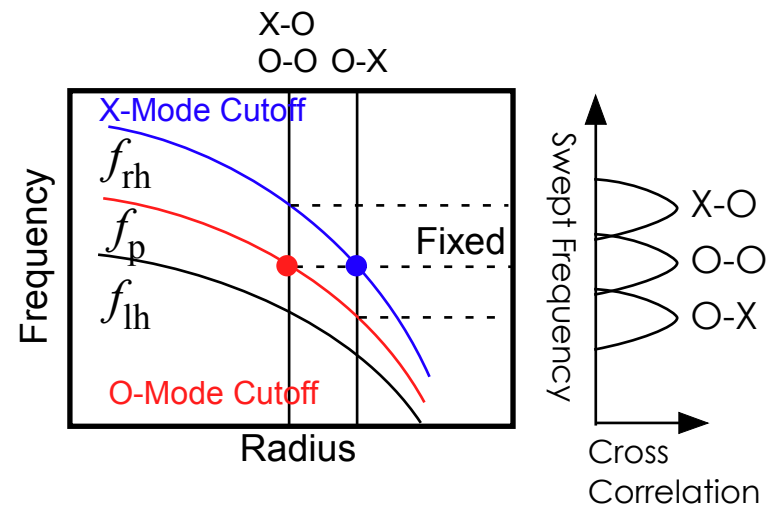
N_x, N_O : indices of refraction

$\phi = d\theta/dz$: magnetic shear

$\theta = \arctan(B_p/B_t), k_0 = \omega/c$

(propagation perpendicular to B_0).

- Maximum cross-correlation when fixed and swept frequencies are reflecting from same location.
- Mode contamination scenarios:
 - Fixed X-mode and swept O-mode (main).
 - Fixed O-mode (main) and swept X-mode.
 - Fixed X-mode and swept X-mode is 2nd order quantity.



Reference:

I. Fidone and G. Granata, Nucl. Fusion 11, 133 (1971).

1-D Full-Wave Code for Evaluation of O-/X-Mode Conversion



Normalized Equations

$$\begin{aligned}\frac{\partial \hat{\mathbf{B}}}{\partial t} &= -\nabla \times \hat{\mathbf{E}} \\ \frac{\partial \hat{\mathbf{E}}}{\partial t} &= \nabla \times \hat{\mathbf{B}} - \hat{\mathbf{J}} \\ \frac{\partial \hat{\mathbf{J}}}{\partial t} &= -\frac{\omega_{ce}}{\omega_0} \hat{\mathbf{J}} \times \mathbf{b} + \frac{\omega_{pe}^2}{\omega_0^2} \hat{\mathbf{E}}\end{aligned}$$

1-D Reduction on Yee Lattice

$$B_x^{n+0.5}(i+0.5) = 0$$

$$B_y^{n+0.5}(i+0.5) = B_y^{n-0.5}(i+0.5) + \frac{\Delta t}{\Delta x} [E_z^n(i+1) - E_z^n(i)]$$

$$B_z^{n+0.5}(i+0.5) = B_z^{n-0.5}(i+0.5) - \frac{\Delta t}{\Delta x} [E_y^n(i+1) - E_y^n(i)].$$

$$E_x^{n+1}(i) = E_x^n(i) - \Delta t \cdot J_x^{n+0.5}(i)$$

$$E_y^{n+1}(i) = E_y^n(i) - \Delta t \cdot J_y^{n+0.5}(i) - \frac{\Delta t}{\Delta x} [B_z^{n+0.5}(i+0.5) - B_z^{n+0.5}(i-0.5)]$$

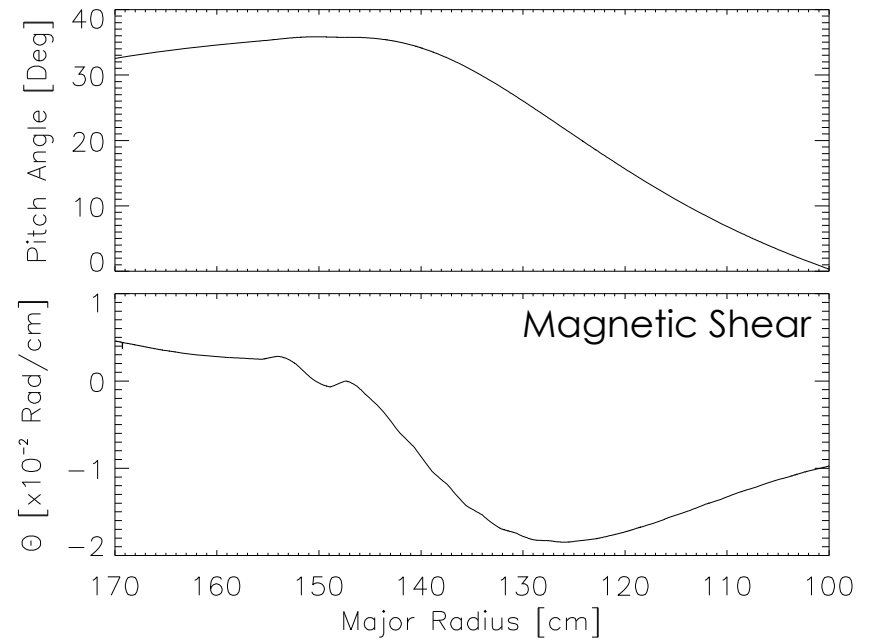
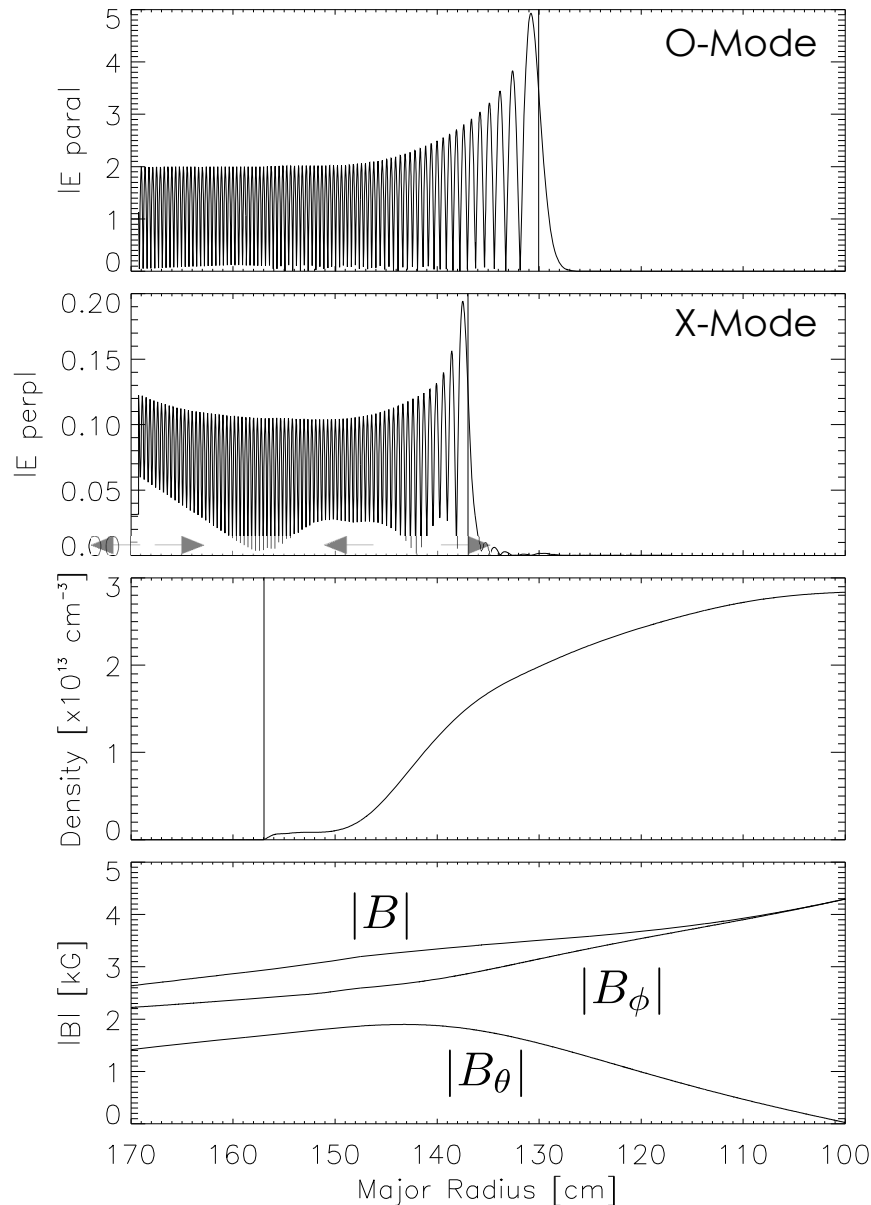
$$E_z^{n+1}(i) = E_z^n(i) - \Delta t \cdot J_z^{n+0.5}(i) + \frac{\Delta t}{\Delta x} [B_y^{n+0.5}(i+0.5) - B_y^{n+0.5}(i-0.5)].$$

$$\begin{bmatrix} 1 & \Delta t \cdot \alpha(i) \cdot b_z(i)/2 & -\Delta t \cdot \alpha(i) \cdot b_y(i)/2 \\ -\Delta t \cdot \alpha(i) \cdot b_z(i)/2 & 1 & \Delta t \cdot \alpha(i) \cdot b_x(i)/2 \\ \Delta t \cdot \alpha(i) \cdot b_y(i)/2 & -\Delta t \cdot \alpha(i) \cdot b_x(i)/2 & 1 \end{bmatrix} \begin{bmatrix} J_x^{n+0.5}(i) \\ J_y^{n+0.5}(i) \\ J_z^{n+0.5}(i) \end{bmatrix} =$$

$$\begin{bmatrix} J_x^{n-0.5}(i) - \Delta t \cdot \alpha(i) \cdot b_z(i) \cdot J_y^{n-0.5}(i)/2 + \Delta t \cdot \alpha(i) \cdot b_y(i) \cdot J_z^{n-0.5}(i)/2 + \Delta t \cdot f(i) \cdot E_x^n(i) \\ J_y^{n-0.5}(i) - \Delta t \cdot \alpha(i) \cdot b_x(i) \cdot J_z^{n-0.5}(i)/2 + \Delta t \cdot \alpha(i) \cdot b_z(i) \cdot J_x^{n-0.5}(i)/2 + \Delta t \cdot f(i) \cdot E_y^n(i) \\ J_z^{n-0.5}(i) - \Delta t \cdot \alpha(i) \cdot b_y(i) \cdot J_x^{n-0.5}(i)/2 + \Delta t \cdot \alpha(i) \cdot b_x(i) \cdot J_y^{n-0.5}(i)/2 + \Delta t \cdot f(i) \cdot E_z^n(i) \end{bmatrix}$$

- Describes simultaneous O- and X-mode propagation in 1-D geometry.
- SF/TF formulation for plane wave source in edge vacuum.
- Mur's 1st order ABC.
- Inputs are electron density, electron temperature, and magnetic field profiles (magnetic shear).
- Cold plasma dispersion relation.
- Typical run parameters:
 - CFL number: 0.5
 - Grid number: 10,000 ($dx = \lambda_{vac}/50$)
 - Time steps: 30,000
- 2-D version of code exists but not practical to run on desktop computer.
- Reference:
 - H. Hojo et al., Rev. Sci. Instrum. 75, 3813 (2004).

Forward & Backward Travelling Waves Generated

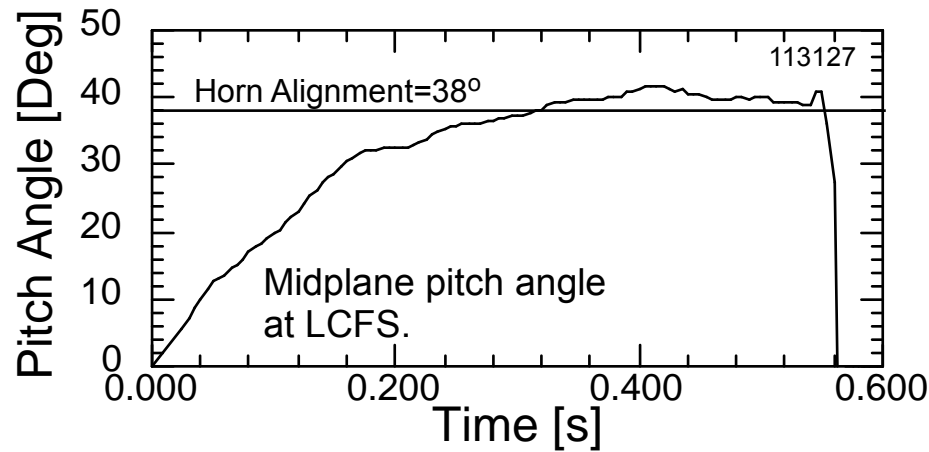


- Profiles from shot 113127, $t=250$ ms. $B_t=4.4$ kG, $I_p=850$ kA, $P_{\text{NB}}=1.0$ MW.
- 40 GHz launch frequency.
- Oscillating standing wave pattern indicates that both forward and backward traveling waves are generated.
- Incident wave amplitude is unity.
- Asymmetry in amplitude of traveling waves.

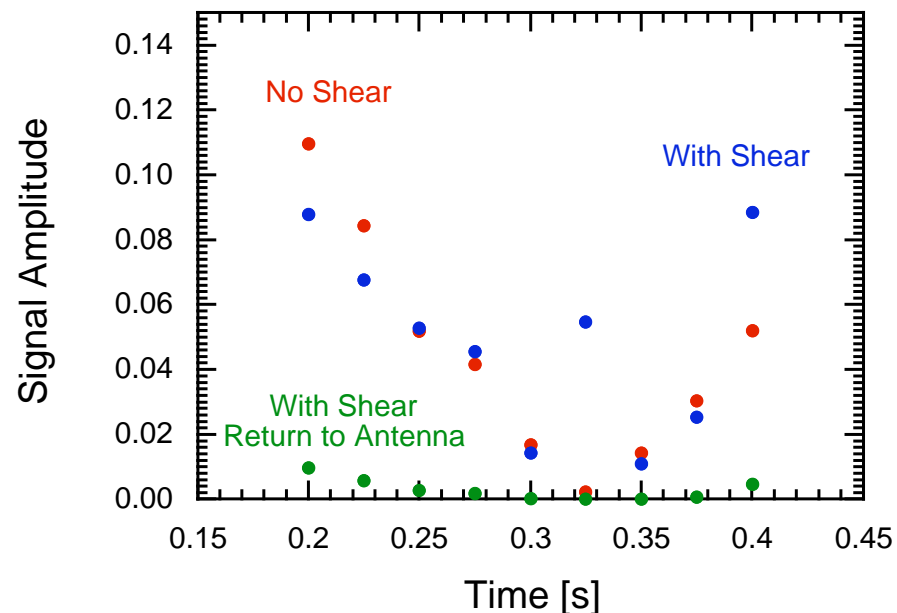
Returning X-Mode Signal Amplitudes and Conclusion



O-Mode Polarization Mismatch with Pitch Angle at the Last Closed Flux Surface



Returning X-Mode Signal (Contamination)



- For typical measurements, polarization of launched/received waves matched fairly well (within 5 degrees) to pitch angle at LCFS.
- Under these conditions, returning X-mode amplitude can range from 1% to 12% of the launched wave amplitude.
- Returning X-mode amplitude can be large (6%) even when polarization matching to pitch angle is good (no X-mode is launched).
- Contamination at antenna is less than 1% and typically less than 0.5%.
- Consistent with the fact that there are no obvious sign of O- and X-mode correlation from fringes (experimental data).

Conclusions:

Signal contamination due to linear mode conversion is not an issue under typical experimental conditions. Assumption of pure O-mode propagation is adequate.

Comparison of Reflectometry Measurements to Simulations



- Interpretation of reflectometry data can be complicated.
 - Dependence on details of plasma profiles.
 - Geometry of diagnostics with respect to plasma.
 - Reflectometer response to turbulence: k , $\delta n/n$, correlation lengths, correlation times, flow velocities.
- Quantitative estimates of turbulence parameters aided by simulations of reflectometer response to modeled turbulence.
 - Application of 2-D PPPL full-wave code to NSTX geometry.
 - Modeled turbulence density correlation function:

$$\frac{\langle \tilde{n}(\mathbf{r}_1) \tilde{n}(\mathbf{r}_2) \rangle}{n(\mathbf{r}_1) n(\mathbf{r}_2)} = \frac{\delta n(\mathbf{r}_1)}{n(\mathbf{r}_1)} \frac{\delta n(\mathbf{r}_2)}{n(\mathbf{r}_2)} \exp \left[- \left(\frac{1}{2} \Delta \mathbf{k} \cdot \Delta \mathbf{r} \right)^2 \right] \cos (\mathbf{k}_m \cdot \Delta \mathbf{r})$$

$\Delta \mathbf{r} = \mathbf{r}_2 - \mathbf{r}_1$ $\delta n/n$: density fluctuation level

$\Delta \mathbf{k}$: wavenumber spread \mathbf{k}_m : wavenumber mean

- Comparison of simulation results with experimental data via coherent reflection:

$$G = \frac{|\langle E \rangle|}{\sqrt{\langle |E|^2 \rangle}}$$

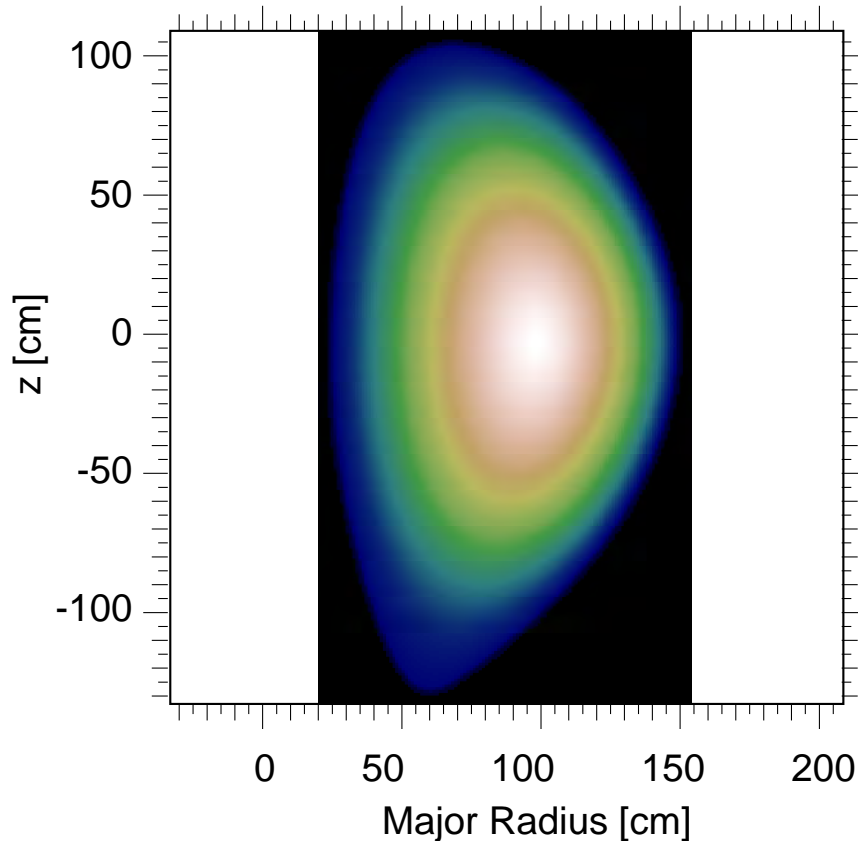
and normalized cross-correlation:

$$\gamma = \frac{|\langle E_1 E_2^* \rangle|}{\sqrt{\langle |E_1|^2 \rangle \langle |E_2|^2 \rangle}}$$

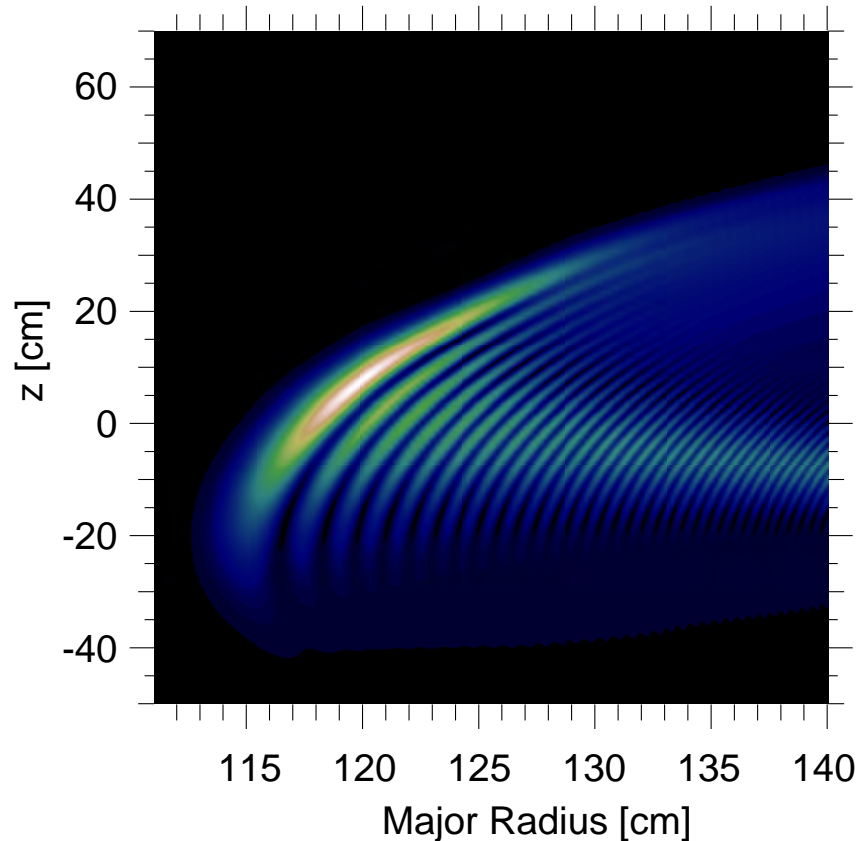
2-D Full-Wave O-Mode Simulations



Density Contours

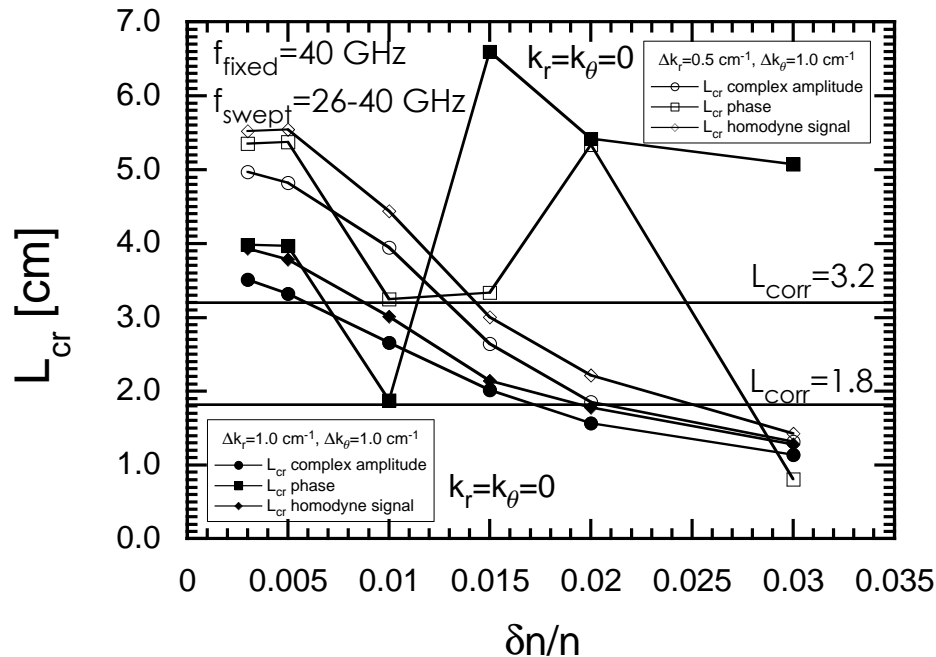
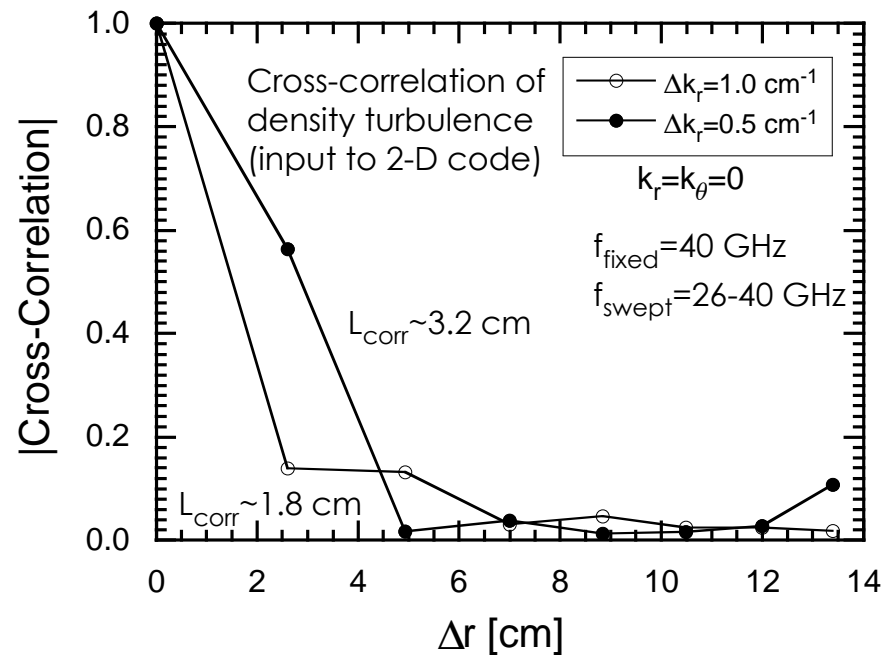
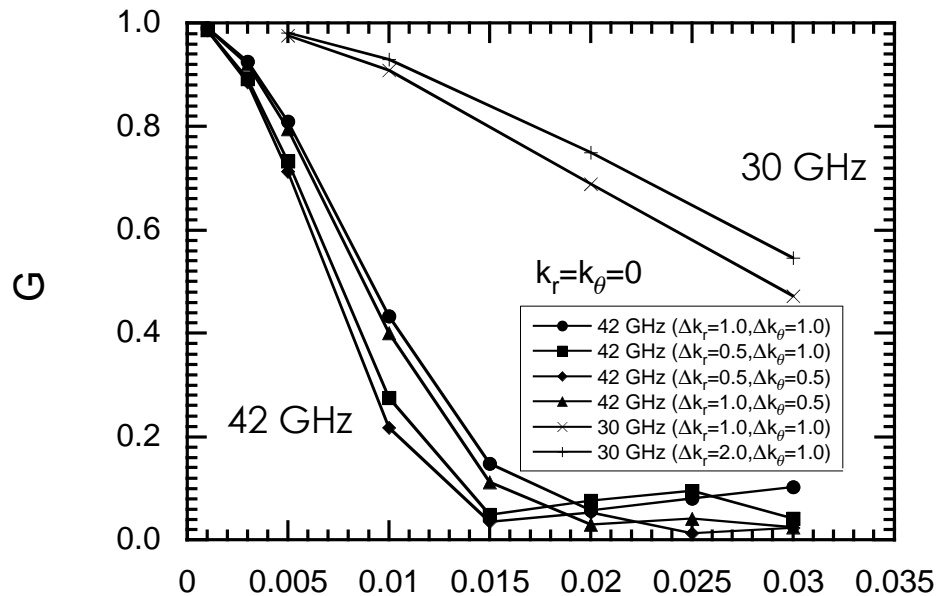


Wave Amplitude for 42 GHz O-Mode



- 2-D density and temperature contours from MPTS and EFIT.
- Launch direction, size, and curvature of incident beam matched to experiment at plasma edge.
- Simulated reflectometer signals calculated from beam pattern of receiving antenna.

G and L_{cr} for Various $\delta n/n$ and Δk



- Shot 113115, $t=330$ ms.
- Comparison of correlation and quadrature reflectometry data with simulations.
- Experimental results:
 $G \sim 0.85$ for 42 GHz, ~ 0.7 for 30 GHz.
 $L_{cr} \sim 11.4 \text{ cm}$
- Homodyne tracks complex amplitude L_{cr} well but overestimates slightly.
- **L_{cr} is strongly dependent on $\delta n/n$.**

Summary and Future Work



- PPPL 2-D full-wave code used to simulate reflectometer response to turbulence.
 - $\delta n/n$ from quadrature measurements.
 - L_{cr} calculated from correlation of homodyne signals can vary significantly from actual turbulence density correlation length. Strongly dependent on $\delta n/n$.
- $\delta n/n$ dependence may explain consistent observation of large correlation lengths (10-20 cm) observed in core.
- Future work:
 - Continue 2-D reflectometry simulations for different plasma conditions. In particular, consider radial variation of turbulence wavenumber spectra and $\delta n/n$.
 - Application of 2-D full-wave code to output from global non-linear gyrokinetic simulations (GYRO).

Correlation Length Measurements During Ohmic H-Modes

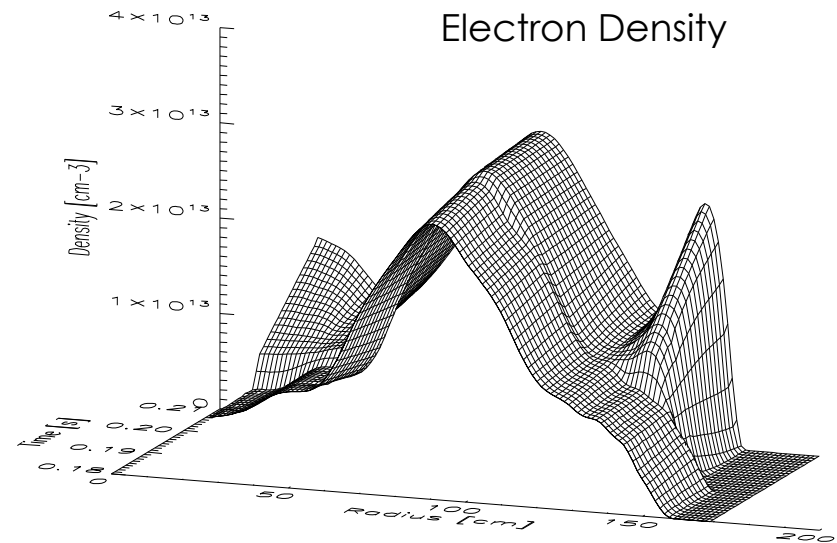
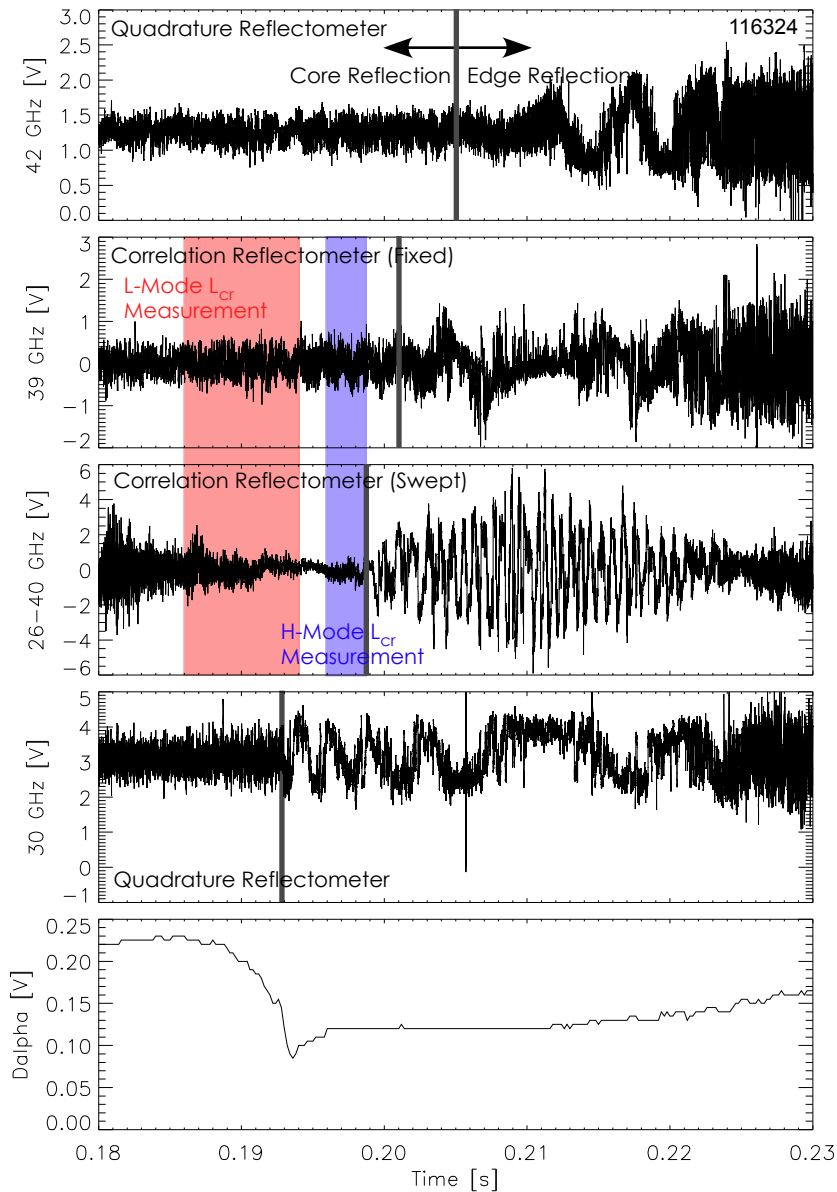


- Motivation:
 - Diagnostics of core properties in H-mode plasmas with reflectometry is difficult.
 - For NB- and HHFW-heated H-mode plasmas, density profile before L-H transition is typically flat (reflectometer cutoffs at edge).
 - No core access before or after L-H transition.
 - Ohmic discharges typically have peaked density profiles (good core access for reflectometers).
- Characteristics of Ohmic H-modes:
 - Low density and peaked L-mode type density profile allows reflectometers to access the plasma core.
 - L-H transition occurs when density is peaked. Edge ears grow, however core profile remains relatively unchanged.
 - Small window of time exists immediately after L-H transition (before edge ear cuts off reflectometer) when core is accessible.

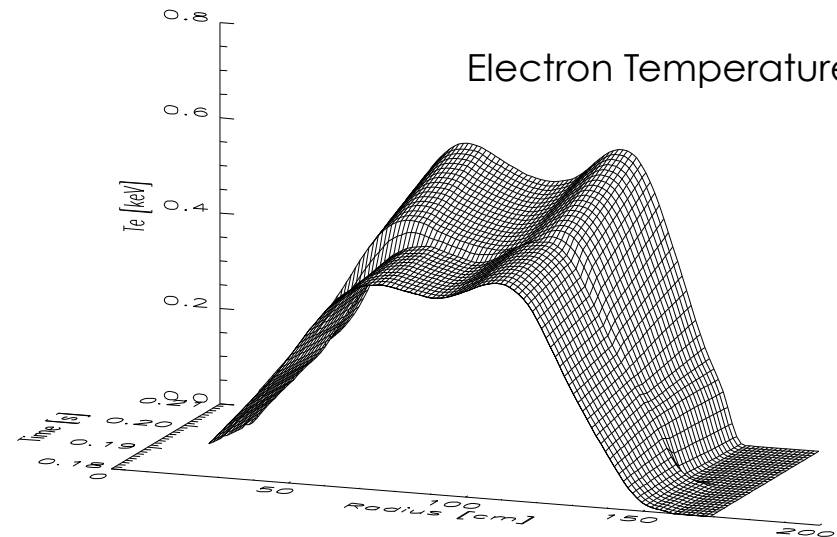
Profile Evolution During Ohmic H-Mode



Reflectometer Raw Signals and Dalphi

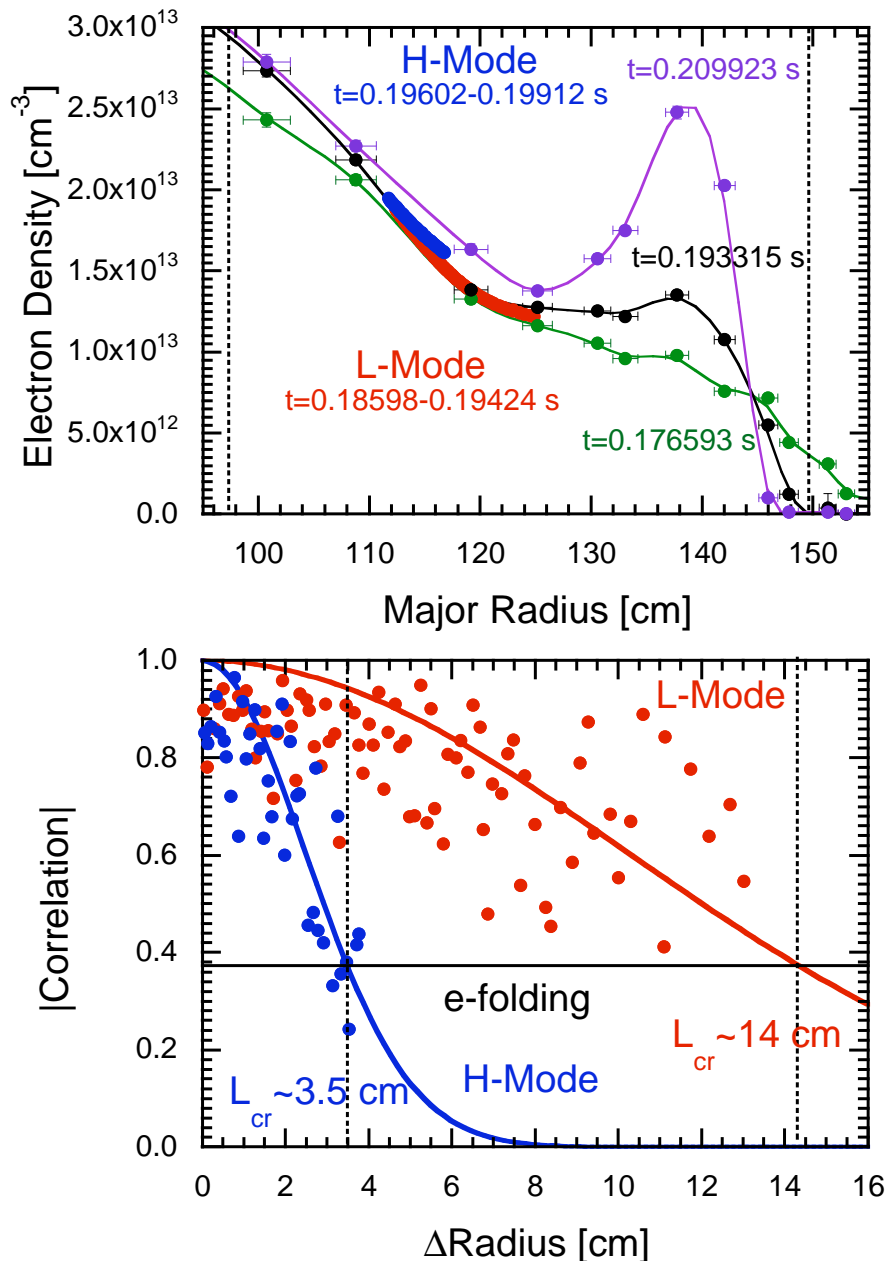


Electron Density

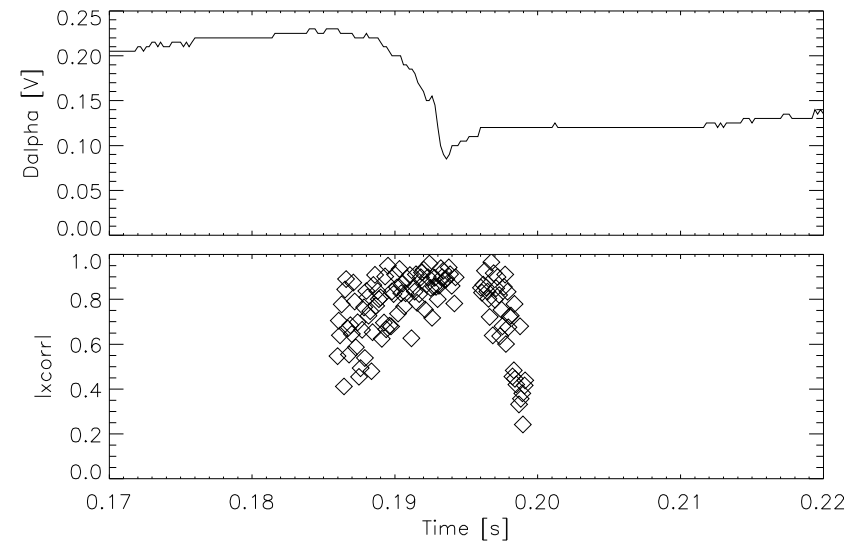


Electron Temperature

Correlation Length Decreases at L-H Transition

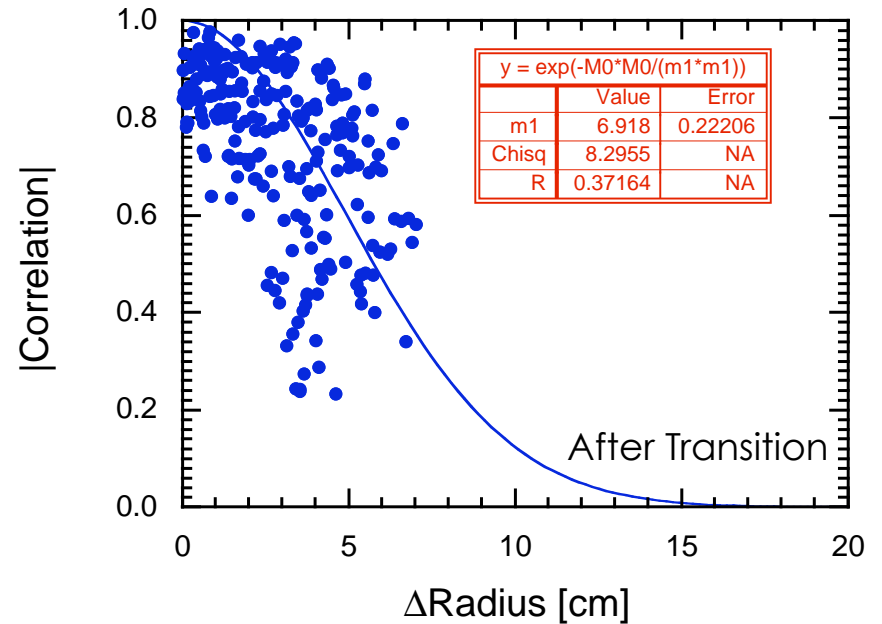
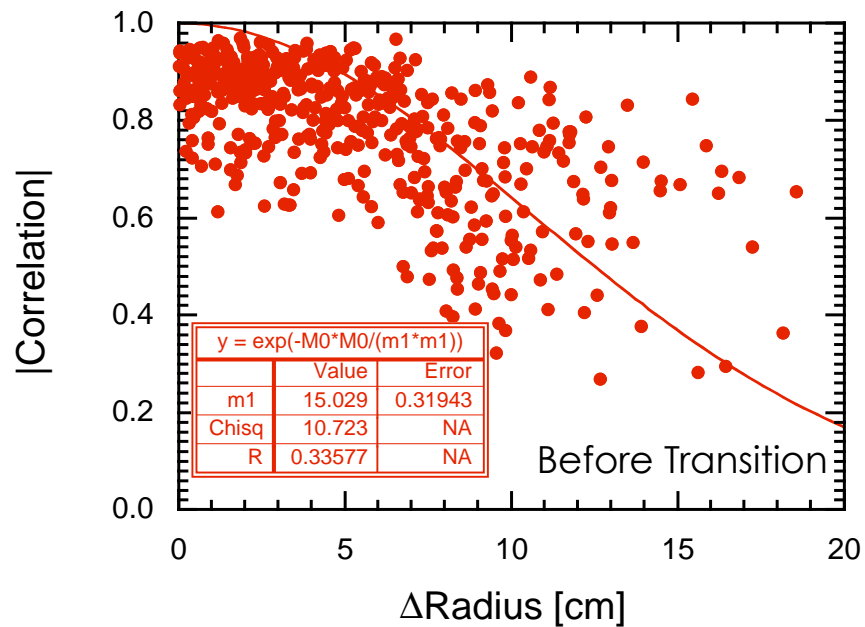


Time series of cross-correlation values near L-H transition.



- Typical L_{cr} drops from $\sim 10-20$ cm to $\sim 4-8$ cm at L-H transition.
- Eventual rise in edge density cuts off reflectometer signal.
- For core 42 GHz channel, statistical properties of signal (amplitude histogram, complex spectrum) remain constant across transition \rightarrow turbulence properties closer to axis changing little.

Correlation Length Decreases By ~1/2 at L-H Transition

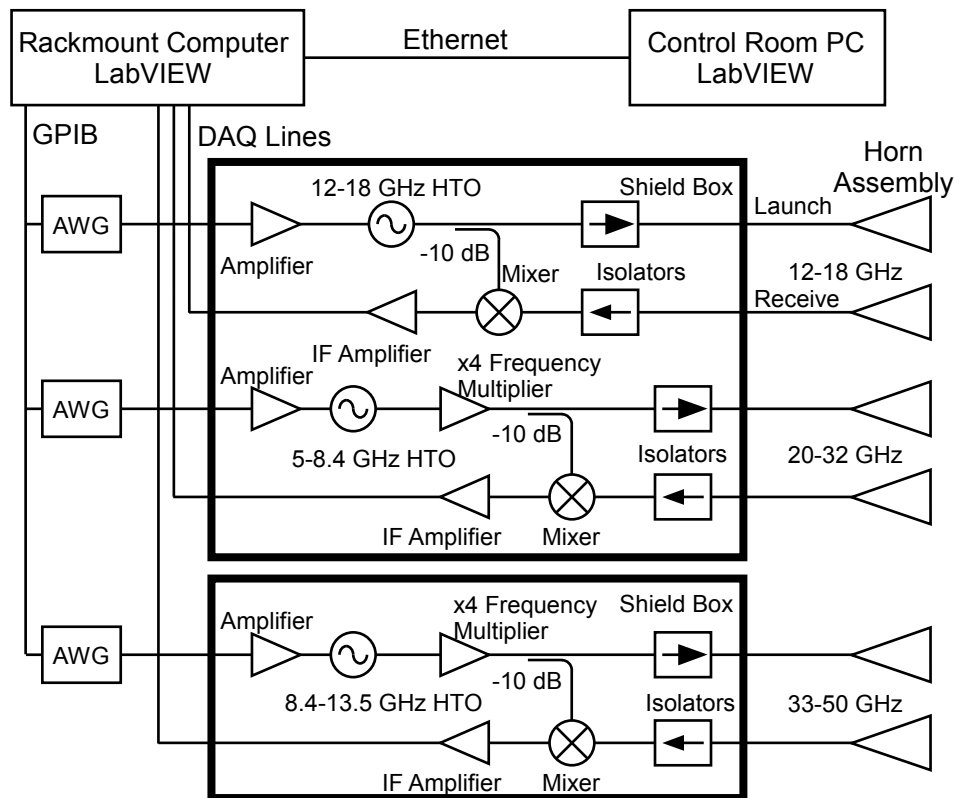


Summary of Ohmic H-mode Results and Future Work



- Change are observed in the core turbulence characteristics across the L-H transition.
 - Correlation lengths at mid-radius in L-mode phase similar to L_{cr} measurements made previously for other discharges ($L_{cr} \sim 10\text{-}20$ cm).
 - At H-mode transition, L_{cr} decreases on average by about 1/2.
 - Decrease in L_{cr} is observed in all ohmic H-mode discharges.
 - Complex amplitude of 42 GHz quadrature reflectometer shows little change at L-H transition (this is deeper in core).
 - N_e and T_e profiles change very little in core at L-H transition.
- Radial decorrelation due to increase in ExB shear?
(See C.E. Bush et al, Poster **RP1 28**)
- Future work:
 - 2-D full-wave simulations to better quantify turbulence characteristics.
 - Poloidal rotation velocities through poloidal correlation measurements of turbulence may help quantify ExB shear.

FMCW Reflectometer System



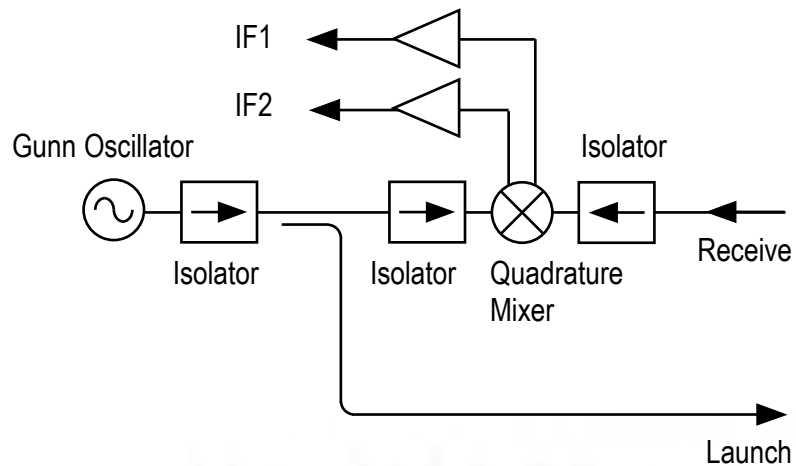
FMCW System

- 13-52 GHz coverage (2.1×10^{12} to $3.4 \times 10^{13} \text{ cm}^{-3}$).
- Maximum repetition rate of 25 $\mu\text{s}/\text{sweep}$ (3840 total profiles per shot).
- Using spline fit to Thomson edge profile below $n_e = 9 \times 10^{11} \text{ cm}^{-3}$.
- Typical discrepancy of less than 1 cm between reflectometry and Thomson scattering profiles. Edge modeling and systematic uncertainties.

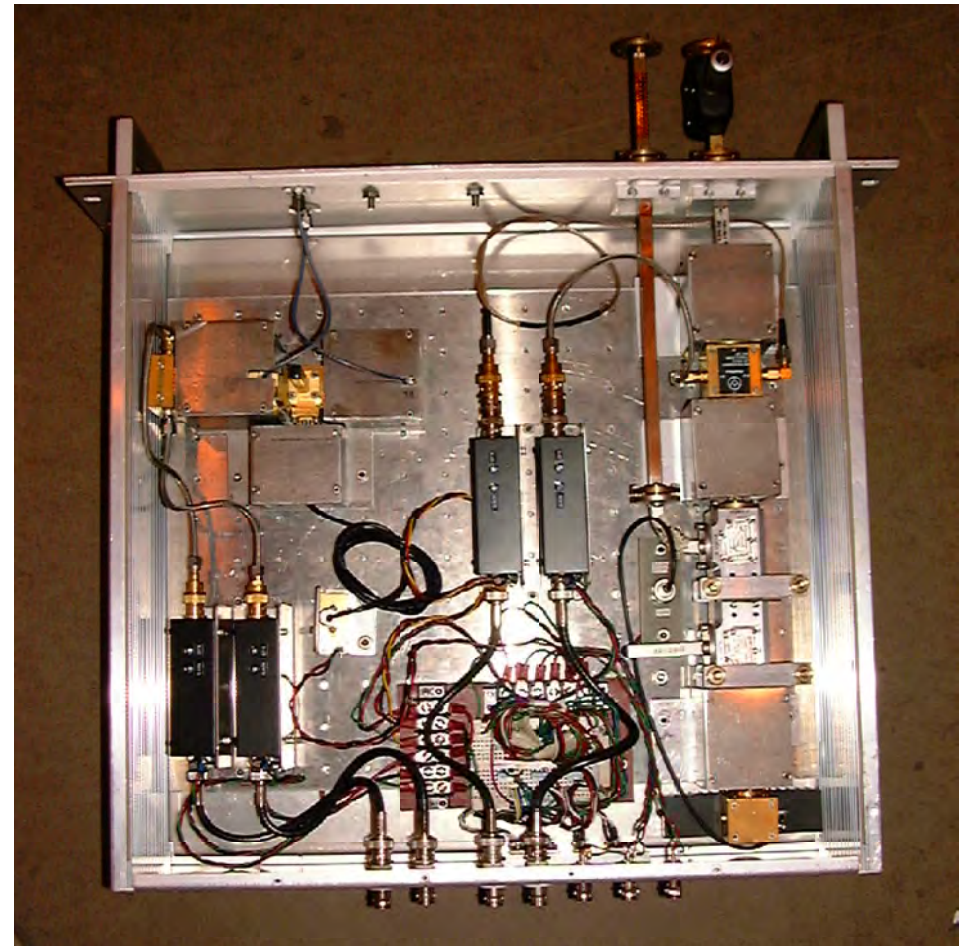
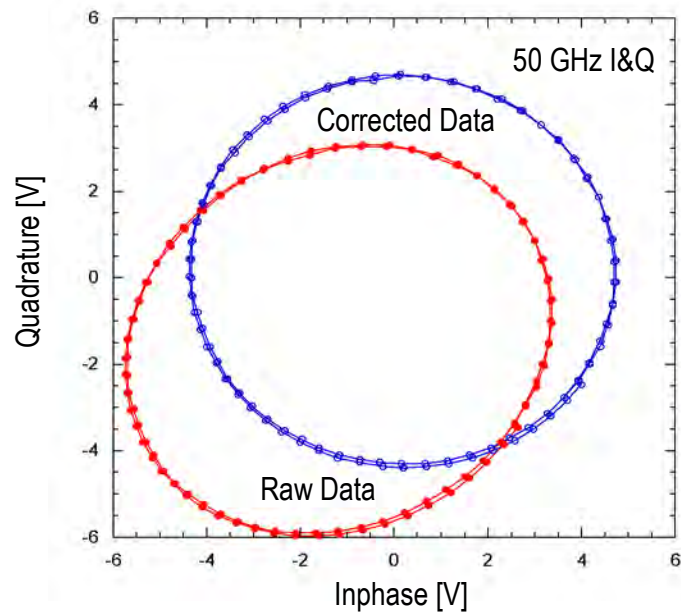
Quadrature Reflectometers



- 50 GHz homodyne quadrature reflectometer circuit.



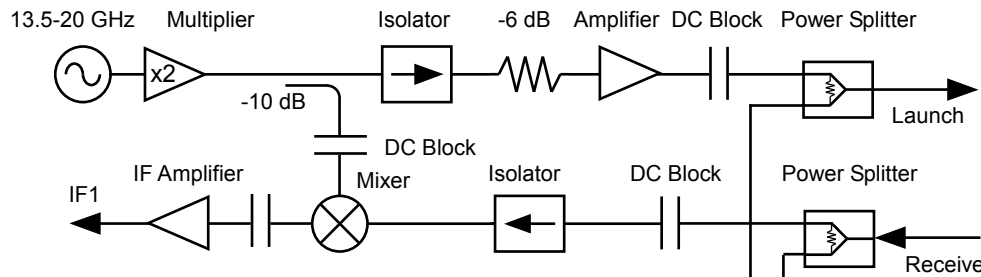
- DC offset, phase and amplitude imbalance corrections.



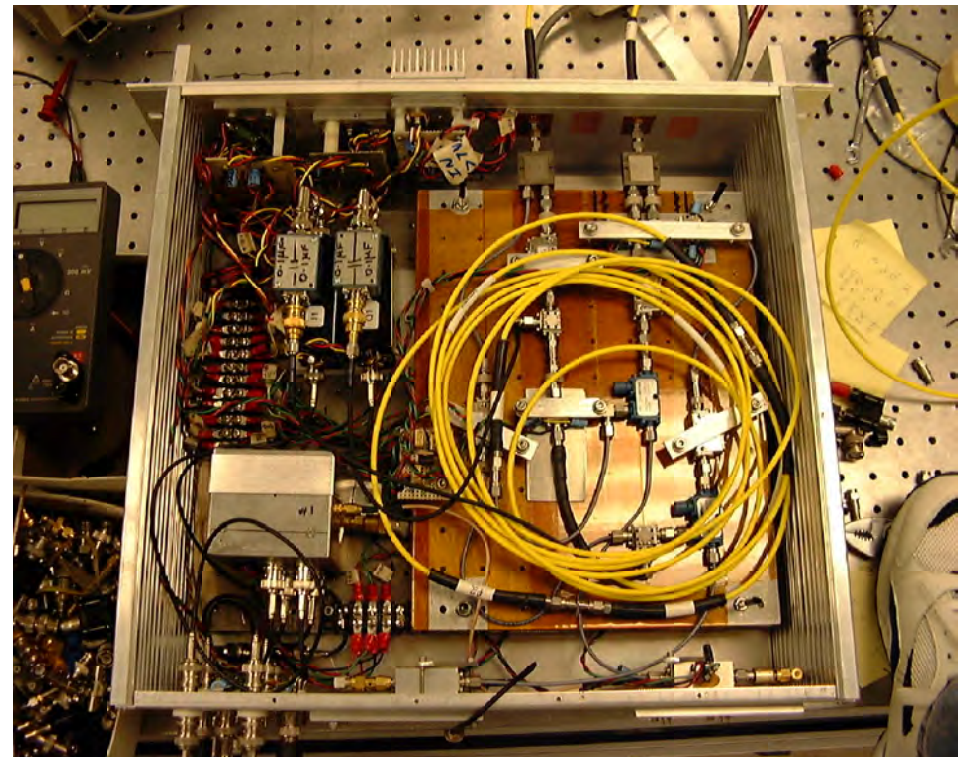
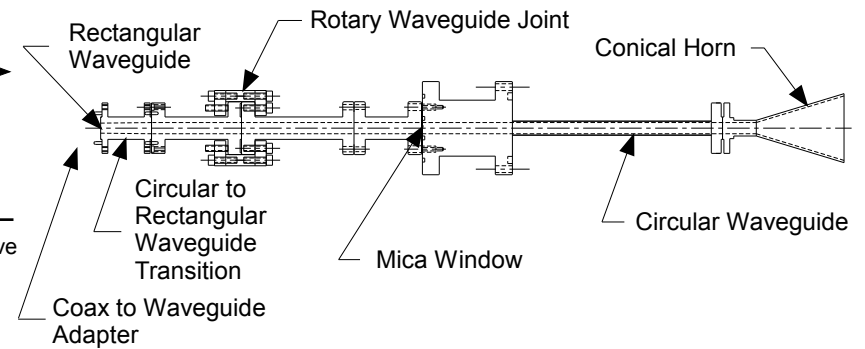
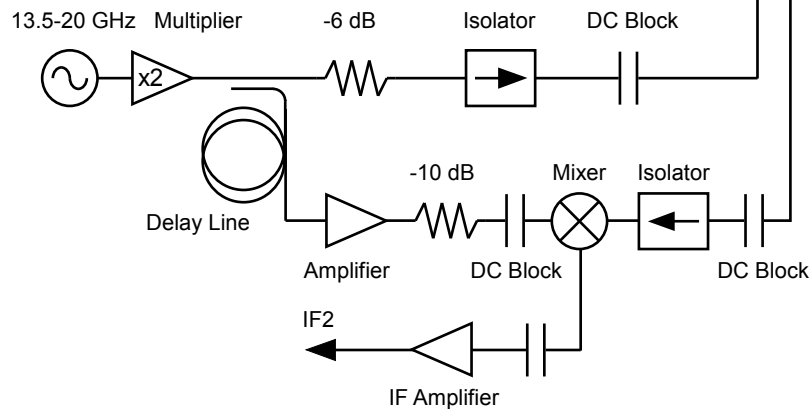
Homodyne Radial Correlation Reflectometer



Fixed Frequency



Swept Frequency

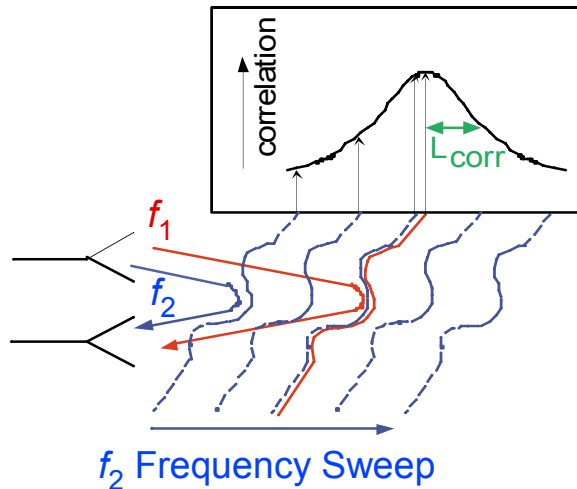


- 26-40 GHz, $n_{cr} \sim 0.85-2.0 \times 10^{13} \text{ cm}^{-3}$.
- Voltage-controlled HTOs for fast sweep rates.
- Both source and DAQ (8 MSa/s) PC-controlled.
- ~14 ft of coaxial cable (roundtrip) between equipment and machine.
- Launch and receive polarization determined via rotary waveguide joint.

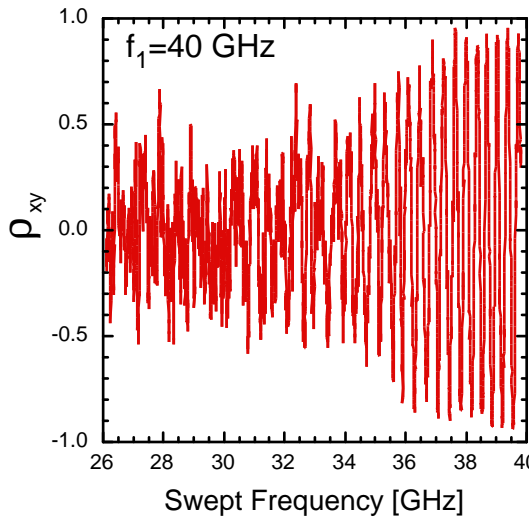
Principle of Homodyne Radial Correlation Reflectometry



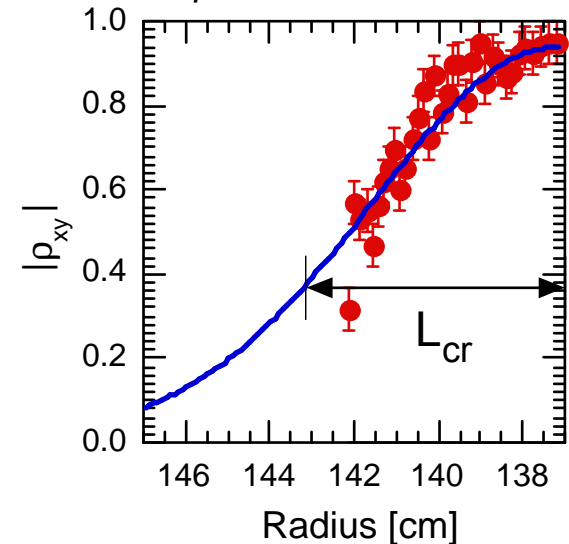
Principle of Radial Correlation Length Measurements



Correlation Coefficient Function vs Swept Frequency



Correlation Coefficient Function Envelope vs Radius



- Fixed frequency f_1 and swept frequency f_2 with identical launch and receive horns reflect from different cutoff layers in the plasma.
- **Correlation coefficient function** of homodyne signals x and y is modulated by the swept DC phase of f_2 .

$$\rho_{xy} = \frac{\langle (x - \langle x \rangle)(y - \langle y \rangle) \rangle}{\sqrt{\langle (x - \langle x \rangle)^2 \rangle} \sqrt{\langle (y - \langle y \rangle)^2 \rangle}}$$

- Envelope of correlation coefficient function mapped from from frequency to radial position using density profiles from Thomson scattering.
- Correlation length L_{cr} is defined here as the e-folding distance of the correlation coefficient function envelope (best fit to Gaussian).

Details of L_{cr} Estimates and Normalizations



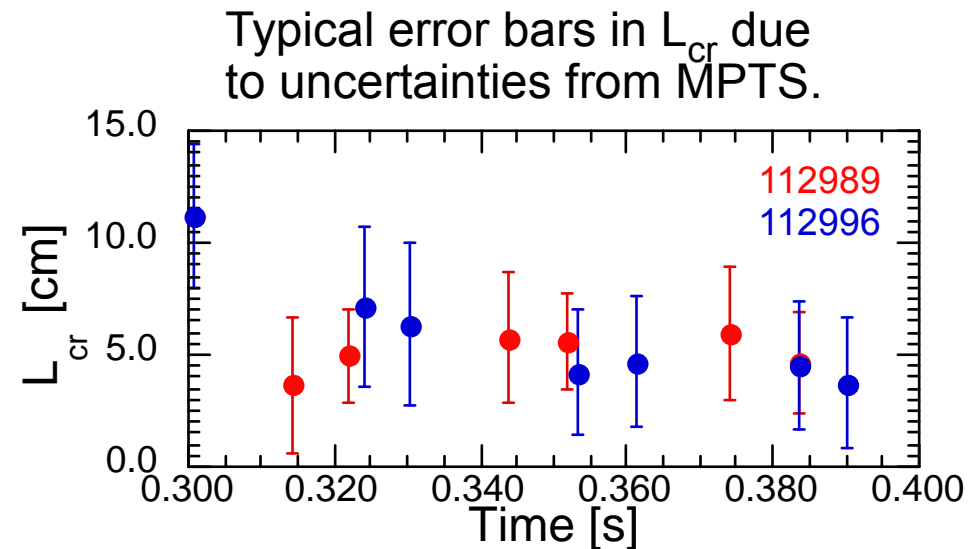
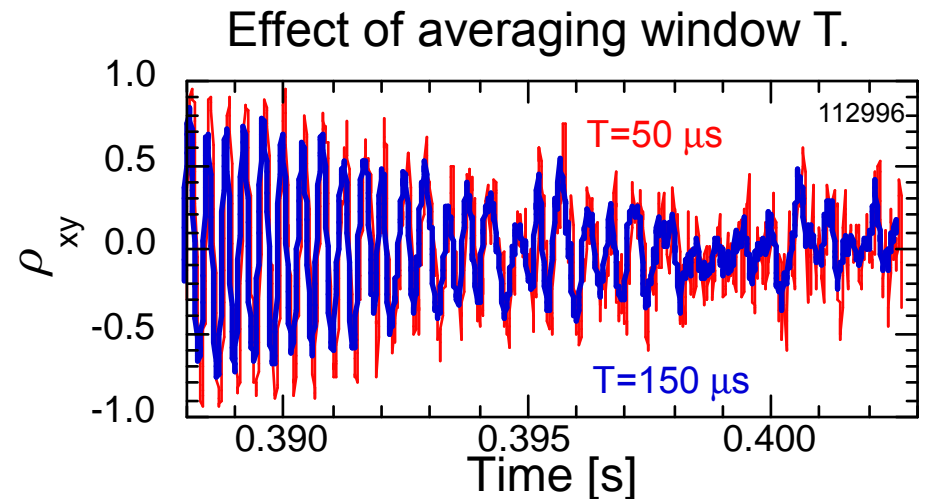
- Averaging window T for ρ_{xy} must be small to catch fringe pattern ($T \sim 50 \mu\text{s}$). Larger T reduces variance but smooths peaks.
- Significant fringe peaks identified by height and spacing.
- Error in L_{cr} can be several cm from uncertainty in MPTS measurements.
- For L_{cr} of several cm, background n_e , T_e , T_i , and B profiles can change significantly over this distance. For gyroradius normalization, these values are taken at the midpoint radius between the the fixed frequency cutoff and the $1/e$ location.

- For L_{cr} estimates, an alternative to ρ_{xy} is the **coherency function** γ_{xy} :

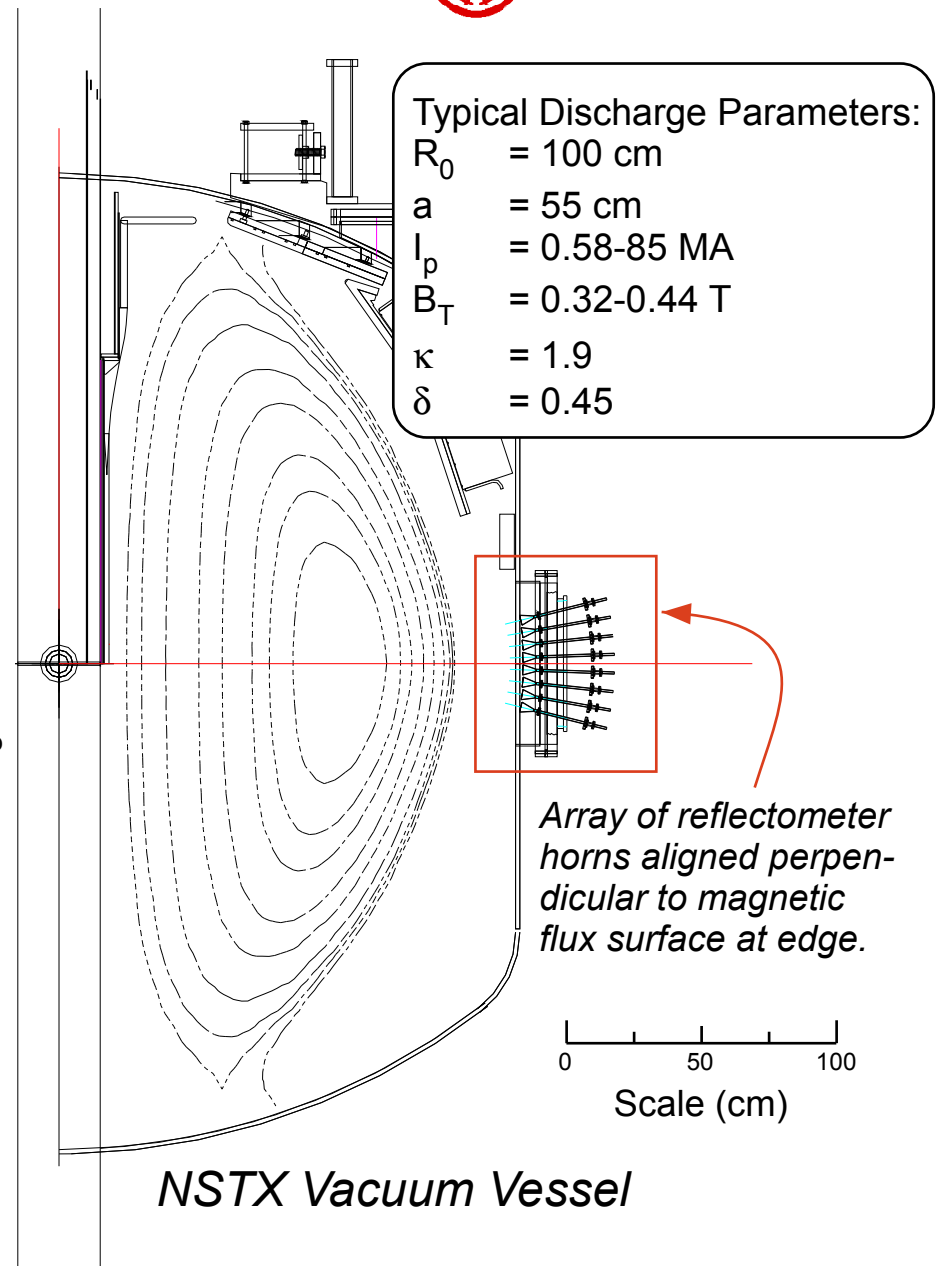
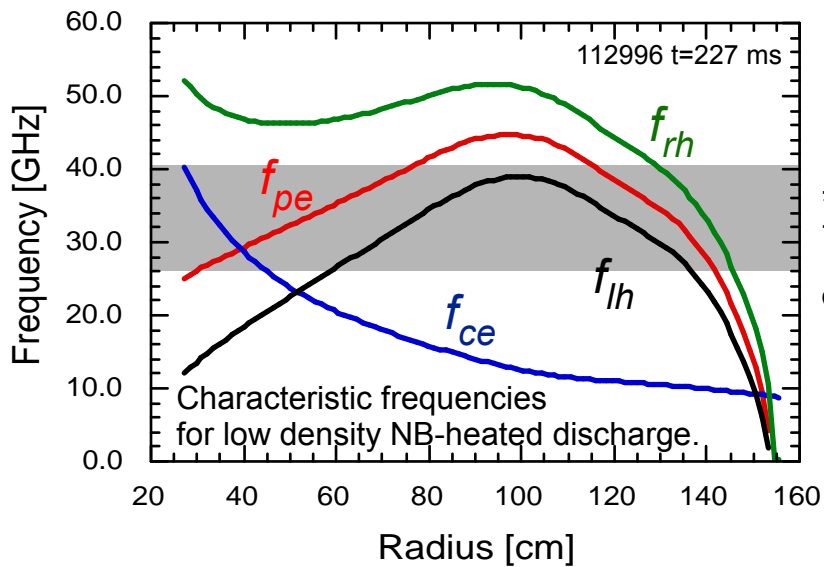
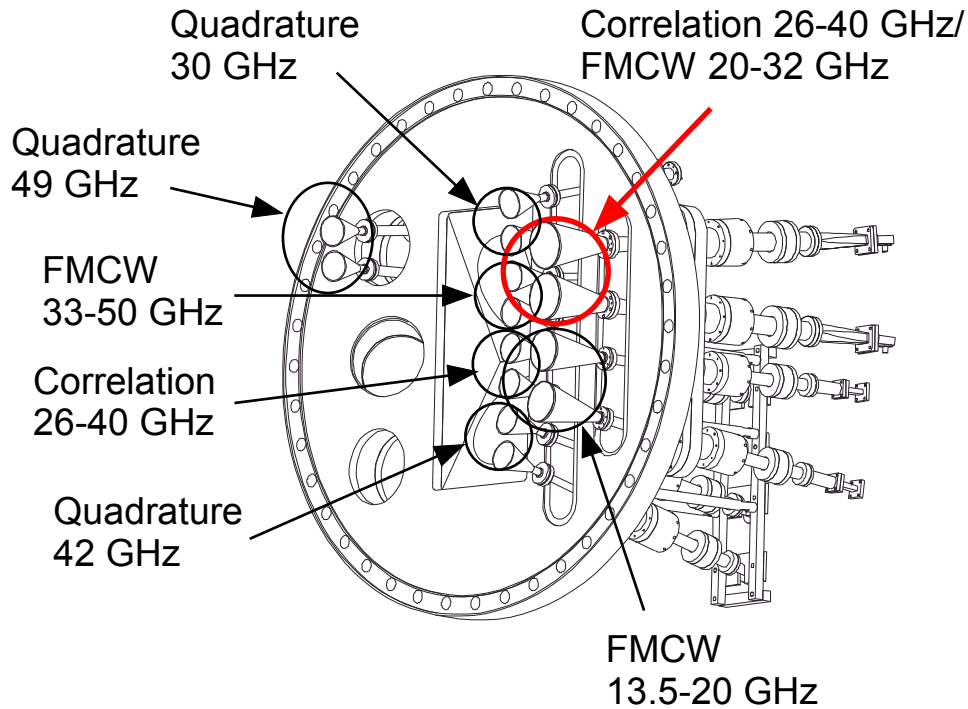
$$\gamma_{xy}^2(f) = \frac{|\langle G_{xy}(f) \rangle|^2}{\langle G_{xx}(f) \rangle \langle G_{yy}(f) \rangle} \quad \bar{\gamma}_{xy}^2 = \frac{\int \gamma_{xy}^2(f) \langle G_{xx}(f) \rangle df}{\int \langle G_{xx}(f) \rangle df}$$

Since good time resolution is required to resolve fringe peaks, ρ_{xy} is used exclusively here.

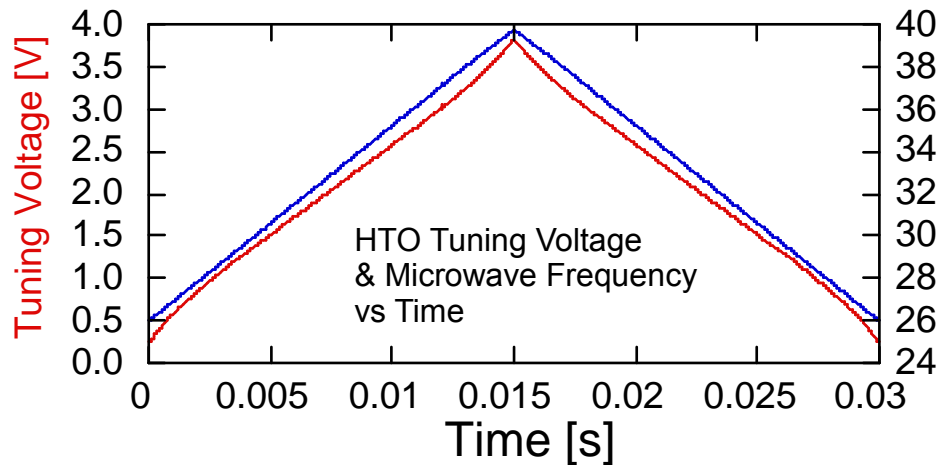
- Airy width $w_{\text{Airy}} = 0.48 L_n^{1/3} \lambda_0^{2/3} \sim 1 \text{ cm}$.



Reflectometer Locations on NSTX



Frequency Sweep Linearization & Path Length Adjustment



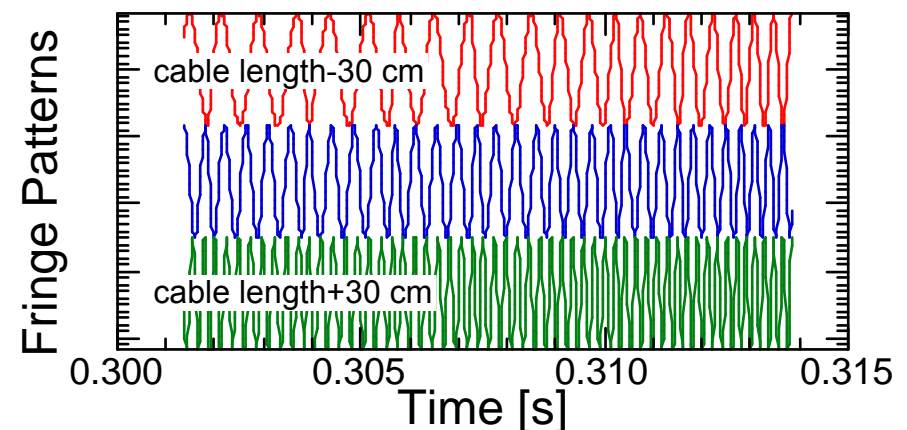
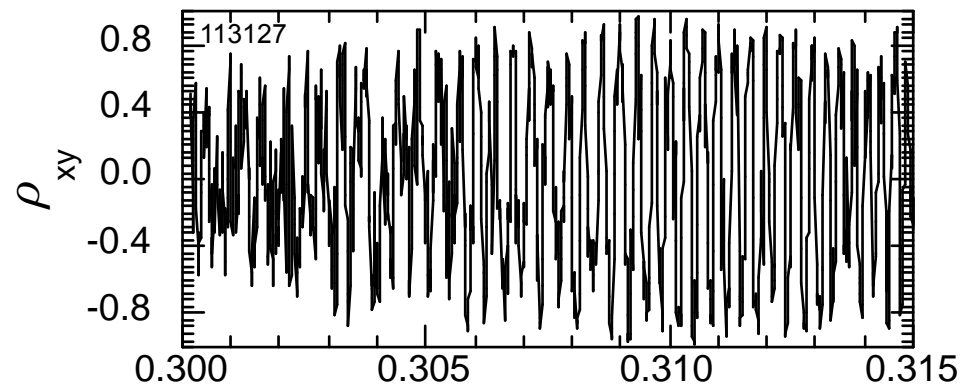
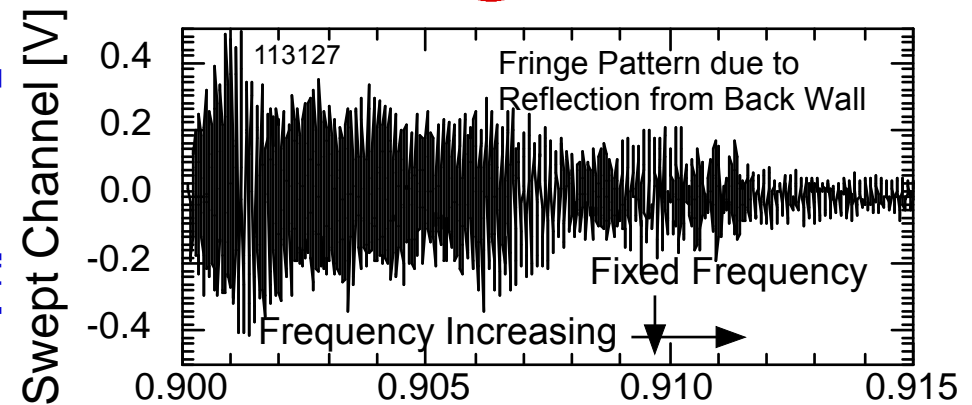
$$\frac{d\phi}{dt} = 2\pi \frac{\Delta L}{c} \frac{df_{\text{rf}}}{dt}$$

ΔL = difference between probe and reference paths
 f_{rf} = microwave frequency
 $\cos \phi$ = fringe pattern of ρ_{xy}

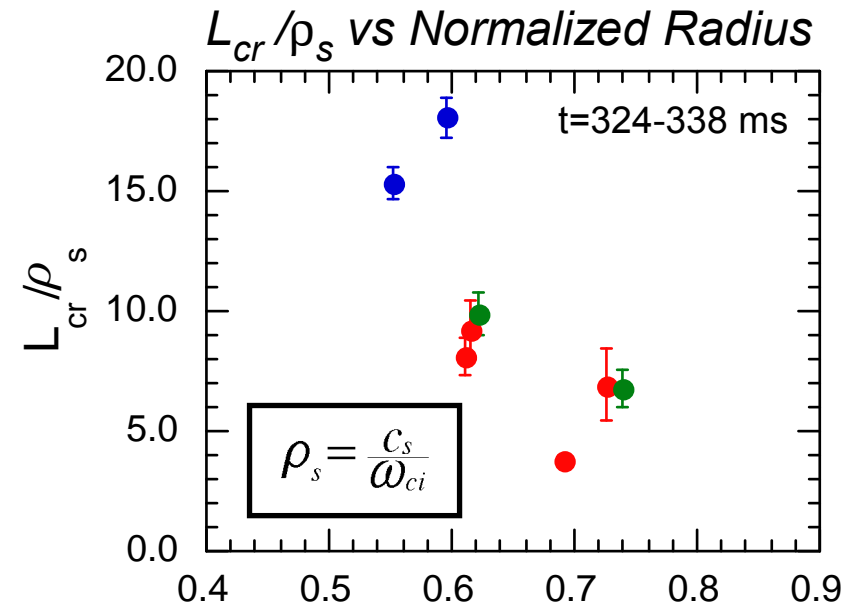
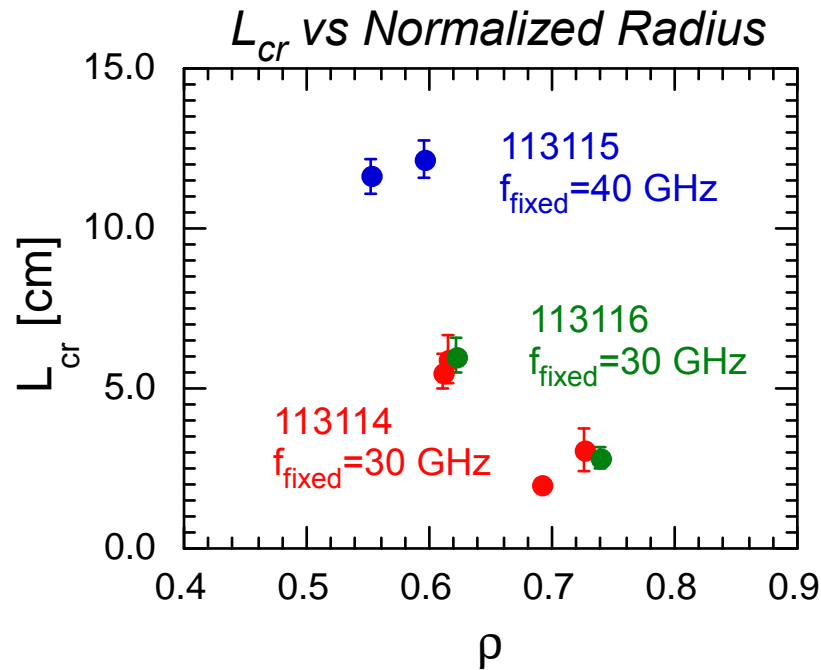
- Reference path length L_r is fixed. Probe path length L_p depends on transmission line (coaxial cable or L_t) and plasma profile.

$$\Delta L(f_{\text{rf}}) = 2 \underbrace{\int_{r_a}^{r_c} \mu(r, f_{\text{rf}}) dr}_{\text{plasma contribution}} + L_t(f_{\text{rf}}) - L_r(f_{\text{rf}})$$

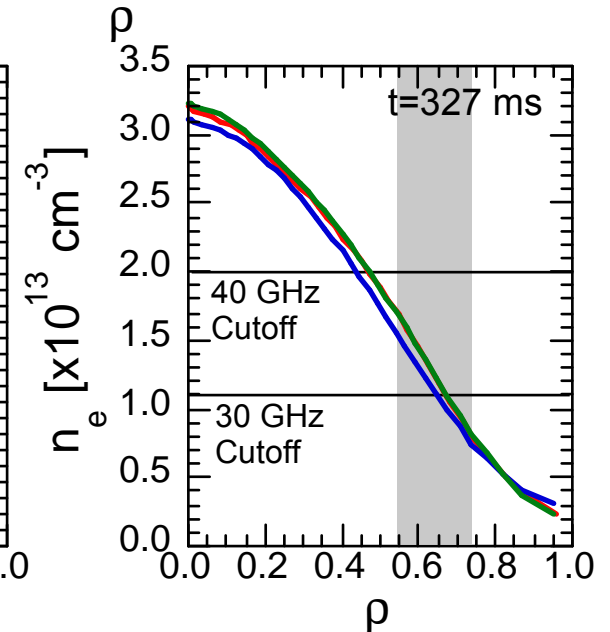
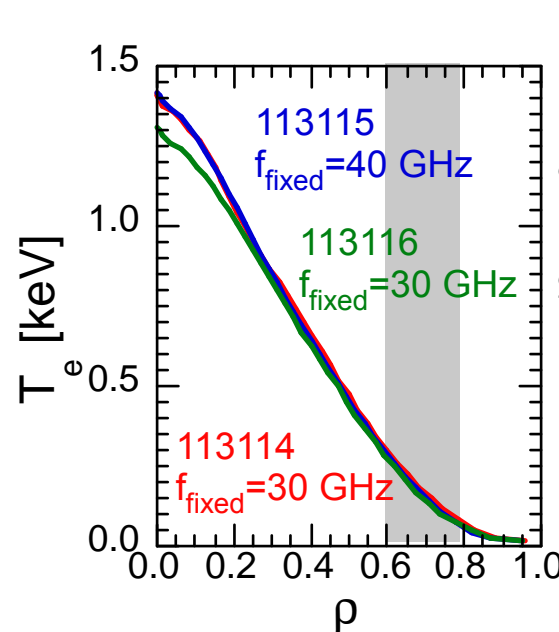
- Number of fringes per full band sweep adjusted by varying cable length.



Radial Scan: $L_{cr} \sim 2-12$ cm at $r \sim 0.55-0.75$



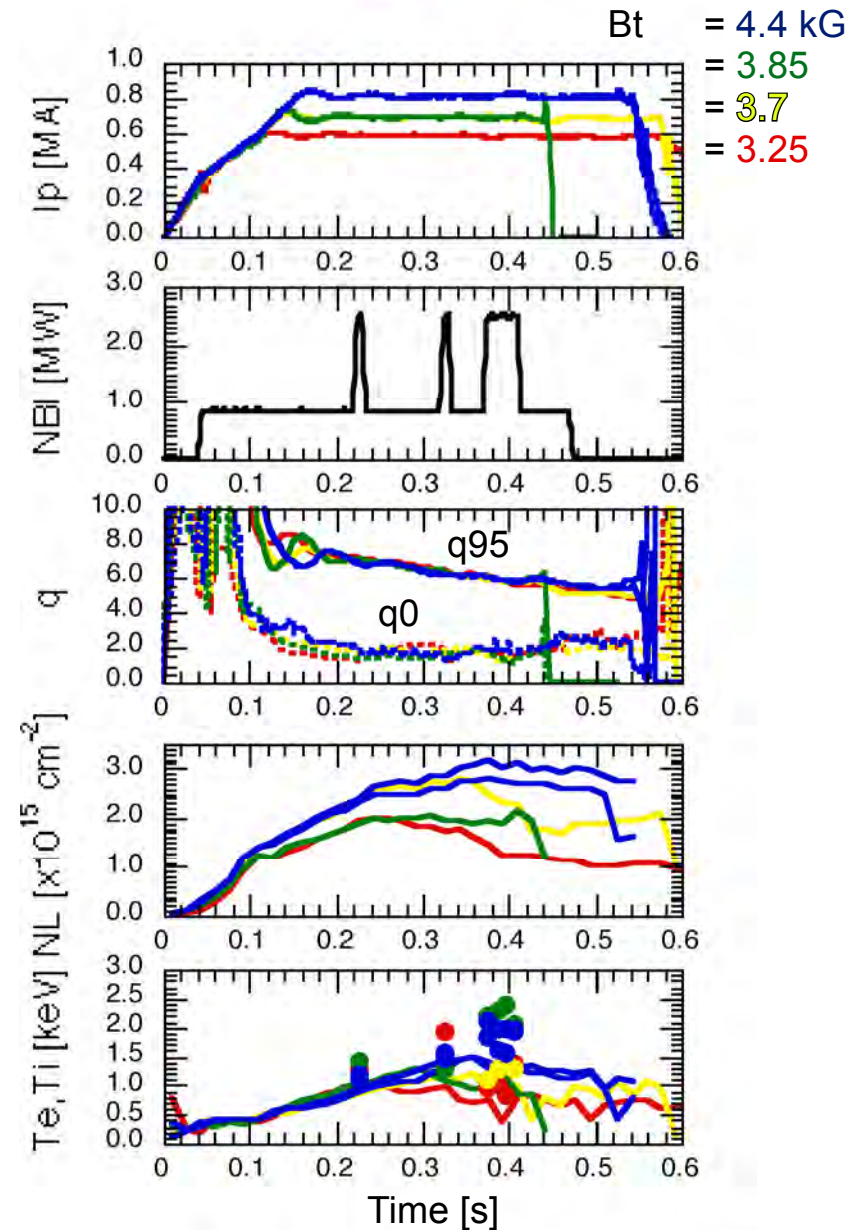
- $B_t=4.4$ kG, $I_p=850$ kA, f_{fixed} at 30 and 40 GHz.
- L_{cr} ranges from 2-12 cm over radius of $\rho \sim 0.55-0.75$.
- L_{cr} increases inversely with ρ .
- L_{cr}/ρ_s varies from 4-18 over this range.



Experimental Conditions for ρ^* Scan



- Various scans were performed:
 - ρ^* scan at constant q : $B_t=3.25-4.4$ kG with corresponding $I_p=580-850$ kA.
 - I_p Scan at fixed $B_t=4.4$ kG: $I_p=680-850$ kA.
 - B_t Scan at fixed $I_p=680$ kA: $B_t=3.7-4.4$ kG.
- Scan of radial location by changing fixed frequency of correlation reflectometer: 30, 35, and 40 GHz ($n_{cr}=1.1, 1.5$ and 2.0×10^{13} cm $^{-3}$).
- Shots with similar profiles at different conditions were difficult to find.
 - At lower B_t , MHD and beam-driven instabilities (fishbones, TAEs, CAEs?) a problem.
 - Collapse of T_e and n_e due to pressure peaking during middle of discharge.
- Three comparisons presented here:
 - ρ^* scan: $B_t=3.7$ and 4.4 kG, $\rho \sim 0.45$ and 0.65.
 - ρ^* scan: $B_t=3.25, 3.85$ and 4.4 kG, $\rho \sim 0.7$.
 - Radial scan for $B_t=4.4$ kG, $I_p=850$ kA.



Sign-Up for Electronic Copy

